NASA/TM—2014–216626

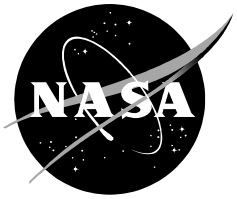

Combined Electric Aircraft and Airspace Management Design for Metro-Regional Public Transportation

Dr. John Melton, Dr. Dean Kontinos, and Dr. Shon Grabbe
Ames Research Center, Moffett Field, California

Jeff Sinsay
U.S. Army Aviation Development Directorate-AFDD (ARMDEC)
Moffett Field, California

Juan J. Alonso and Brendan Tracey
Stanford University, Stanford, California

October 2014

NASA STI Program ... in Profile

Since its founding, NASA has been dedicated

to the advancement of aeronautics and space science. The NASA scientific and technical information (STI) program plays a key part in helping NASA maintain this important role.

The NASA STI program operates under the auspices of the Agency Chief Information Officer. It collects, organizes, provides for archiving, and disseminates NASA's STI. The NASA STI program provides access to the NTRS Registered and its public interface, the NASA Technical Reports Server, thus providing one of the largest collections of aeronautical and space science STI in the world. Results are published in both non-NASA channels and by NASA in the NASA STI Report Series, which includes the following report types:

- TECHNICAL PUBLICATION. Reports of completed research or a major significant phase of research that present the results of NASA Programs and include extensive data or theoretical analysis. Includes compilations of significant scientific and technical data and information deemed to be of continuing reference value. NASA counterpart of peer-reviewed formal professional papers but has less stringent limitations on manuscript length and extent of graphic presentations.

- TECHNICAL MEMORANDUM. Scientific and technical findings that are preliminary or of specialized interest, e.g., quick release reports, working papers, and bibliographies that contain minimal annotation. Does not contain extensive analysis.

- CONTRACTOR REPORT. Scientific and technical findings by NASA-sponsored contractors and grantees.

- CONFERENCE PUBLICATION. Collected papers from scientific and technical conferences, symposia, seminars, or other meetings sponsored or co-sponsored by NASA.

- SPECIAL PUBLICATION. Scientific, technical, or historical information from NASA programs, projects, and missions, often concerned with subjects having substantial public interest.

- TECHNICAL TRANSLATION. English-language translations of foreign scientific and technical material pertinent to NASA's mission.

Specialized services also include organizing

and publishing research results, distributing specialized research announcements and feeds, providing information desk and personal search support, and enabling data exchange services.

For more information about the NASA STI program, see the following:

- Access the NASA STI program home page at http://www.sti.nasa.gov

- E-mail your question to help@sti.nasa.gov

- Phone the NASA STI Information Desk at 757-864-9658

- Write to:
  NASA STI Information Desk
  Mail Stop 148
  NASA Langley Research Center
  Hampton, VA 23681-2199

NASA/TM—2014–216626

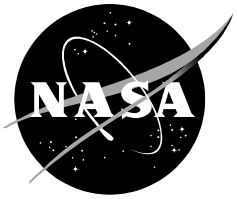

Combined Electric Aircraft and Airspace Management Design for Metro-Regional Public Transportation

Dr. John Melton, Dr. Dean Kontinos, and Dr. Shon Grabbe
Ames Research Center, Moffett Field, California

Jeff Sinsay
U.S. Army Aviation Development Directorate-AFDD (ARMDEC)
Moffett Field, California

Juan J. Alonso and Brendan Tracey
Stanford University, Stanford, California

National Aeronautics and
Space Administration

Ames Research Center
Moffett Field, CA 94035-1000

October 2014

Acknowledgments

The authors are grateful to the NASA Aeronautics Research Mission Directorate (ARMD) Seedling Fund and the NASA Aeronautics Research Institute (NARI) for the support of this study, and to Larry Young and Heather Arneson, NASA Ames Research Center, for technical editing and input into this report.

Available from:

NASA Center for AeroSpace Information
7115 Standard Drive
Hanover, MD 21076-1320
443-757-5802

National Technical Information Service
5301 Shawnee Road
Alexandria, VA 22312
703-605-6000

Table of Contents

Table of Contents (cont.)

List of Figures

List of Figures (cont.)

List of Tables

Nomenclature

AGL	above ground level
AHS	American Helicopter Society
AR	aspect ratio
ARMD	(NASA) Aeronautics Research Mission Directorate
ARTCC	Air Route Traffic Control Center
ATM	Air Traffic Management
BART	Bay Area Rapid Transit
b_k	aircraft-type passenger capacity; employed in network topology (fleet assignment/optimization) analysis
C	C-rate; rate a battery is discharged relative to its maximum capacity
CEO	Chief Executive Officer
$C_{f,k}$	flight costs; employed in network topology (fleet assignment/optimization) analysis
CO_2	carbon dioxide
CONOPS	concept of operations
4-D	four-dimensional
DES	Discrete Event Simulation
$D_{h,k}$	cost of a repositioning flight; employed in network topology (fleet assignment/optimization) analysis
DL	rotor disk loading, DL=T/A, i.e. rotor thrust, T, divided by rotor disk area, A
DOC	direct operating cost
E_{batt}	estimated total energy required to be supplied by batteries during mission/flight
f	f'th flight; employed in network topology (fleet assignment/optimization) analysis
F	set of flights; employed in network topology (fleet assignment/optimization) analysis
FACET	Future ATM Concepts Evaluation Tool (NASA-developed)
FAP	(NASA ARMD) Fundamental Aeronautics Program
FSM	finite state machine
$G_{n,k,t}$	number of aircraft of any given type, k, on the ground at a station, n, at any given time, t; employed in network topology (fleet assignment/optimization) analysis
H	set of repositioning flights; employed in network topology (fleet assignment/optimization) analysis
HIGE	hover in ground effect
HOGE	hover out of ground effect
HTS	high temperature superconducting (electric motors)

Nomenclature (cont.)

IFR	Instrument Flight Rules
k	k'th fleet member; employed in network topology (fleet assignment/optimization) analysis
K	set of aircraft types; employed in network topology (fleet assignment/ optimization) analysis
LCC	life-cycle cost
L/D_e	effective lift-to-drag ratio for vehicle in cruise
Li-ion	lithium ion
Li-po	lithium polymer
Li-S	lithium sulfur
MBD	minutes between departures
nm	nautical miles
N	total number of stations in network; employed in network topology (fleet assignment/optimization) analysis
NCT	Northern California Terminal Radar Approach Control
NDARC	NASA Design and Analysis of Rotorcraft (conceptual design software tool)
NH_3	ammonia
OAK	Oakland International Airport
O-D	origin-destination
OEI	one-engine-inoperative
P_{acc}	power required for vehicle accessories
PASS	Program for Aircraft Synthesis Studies
P_{batt}	required power from batteries
p_f	demand for a flight; employed in network topology (fleet assignment/optimization) analysis
P_{motor}	maximum continuous power required for an individual electric motor (kW)
P_{rotor}	required rotor(s) power
psf	pounds per square foot
PST	Pacific Standard Time
PX	passengers
RW	(NASA ARMD FAP) Rotary-Wing project
SFO	San Francisco International Airport
SJC	San Jose International Airport

Nomenclature (cont.)

$S_{n,t}$	constant to indicate whether a takeoff or departure has occurred at time, t; employed in network topology (fleet assignment/optimization) analysis
SoA	state of the art (electric motors)
STOL	short takeoff and landing
T	time of last aircraft departure of the day; employed in network topology (fleet assignment/optimization) analysis
TOGW	takeoff gross weight
TRL	technology readiness level
UTC	Universal Time Coordinated
VFR	visual flight rules
VTOL	vertical takeoff and landing
W_{batt}	estimated weight of batteries
W_k	ownership cost; employed in network topology (fleet assignment/optimization) analysis
W_{motor}	weight of electric motor (lb_f)
χ_{batt}	battery specific energy
XMSN	transmission
$y_{f,k}$	binary decision variable as to flying a flight; employed in network topology (fleet assignment/optimization) analysis
$z_{h,k}$	repositioning flight variable; employed in network topology (fleet assignment/optimization) analysis
η_{batt}	battery efficiency
η_{motor}	electric motor efficiency
η_{ve}	Power electronics (electric power conversion and conditioning) efficiency

Executive Summary

The goal of this initial study was to determine the feasibility of using electric, short or vertical takeoff and landing (STOL or VTOL) vehicles to serve a significant portion of a metro-regional transportation system. To accomplish this goal, an integrated system simulation was developed that incorporated models of compatibly designed aircraft, stations, fleet operations, and airspace. A baseline system simulation was achieved. It incorporated a newly developed discrete event simulator, modified network optimization algorithms, new electric propulsion modules in NASA's Design and Analysis of Rotorcraft (NDARC) tool, and use of the NASA Future ATM Concepts Evaluation Tool (FACET) airspace simulation software to make assessments of possible air traffic conflicts. Key findings from this study were: 1) system and aircraft designed for extreme short-haul (defined as less than 100 miles per flight leg) could be used to serve tens of thousands of daily commuters in a metropolitan area (the nominal throughput was found to be achievable), 2) feasible aircraft designs are possible using conventional turboshaft-engine propulsion and today's technology, 3) VTOL aircraft designs (specifically helicopter configurations) using electric propulsion will be possible in 10–15 years, with larger vehicles possible in 20–30 years, and 4) such aircraft supporting a metro-regional aerial transportation system would likely need to fly below 5,000 feet to minimize airspace conflict with commercial air traffic.

I. Introduction

A novel aircraft (with both conventional and electric propulsion) and airspace management system is being conceptually designed to provide metro-regional transportation capability: notionally a subway or commuter rail system in the sky. The unique aspect of this study is the simultaneous conceptual design of a compatible suite of aircraft, a realistic daily flight schedule, and an airspace system that efficiently and safely transports large numbers of commuters over short distances (less than 100 miles), within a small metro-regional network of stations (or "vertiports"), at low cruise altitudes (less than 5,000 feet). The objective of this study is to determine the technical feasibility of aircraft to provide a solution to regional mass transportation; a capability currently achieved through road and rail. A compelling aspect is that air-connected nodes (station stops) could be dropped, added, or reconnected to suit real-time traffic needs—a feature impossible to attain with a rail system.

The study directly addresses NASA's strategic goals to advance aeronautics research for societal benefit. Transportation is a first-order driver of the economy; an adaptive metropolitan aerial transportation system would have a first-order effect on regional economies and direct economic benefit to the nation. This approach is in contrast to other studies such as those that: 1) use existing aircraft over short-haul routes in conventional flight patterns; 2) use one- or two-passenger personal air vehicles flying free-form point-to-point; or 3) use two- to four-passenger suburban aircraft with short runway capability employing so-called "pocket" airports (ref. 1).

This study ultimately focuses on rotorcraft (helicopters) as the aerial vehicle most compatible with the envisioned metro-regional aerial transportation system. This study is hardly the first time that rotorcraft have been considered (fig. 1)—and even in some cases in the past, implemented (refs. 2-4)—for metro-regional transportation; but it is the first to simultaneously consider the implications of novel network and airspace system management considerations, as well as the operational and technological implications of aerial vehicles supporting a transportation system that embodies electric propulsion.

Figure 1. Hughes Helibus concept circa 1967 (image courtesy of AHS International).

The main objectives of this study are to: 1) develop a number of aircraft conceptual designs that include the power and propulsion system (with both conventional turboshaft and electric propulsion); 2) make an initial assessment of some of the technological and operational challenges of developing aerial vehicle stations (vertiports) that incorporate designs for rapid recharging; 3) develop initial concepts for a routing/airspace system over a representative metropolitan area; 4) identify the dominant factors that drive the design and technology targets to enable critical capabilities; and 5) create a simulation capability that enables analysis of future novel system attributes such as dynamic fleet constitution. A key element of the study was the development of an integrated metro-regional aerial transportation system simulation that incorporates models of compatibly designed aircraft, stations, and local airspace. All of this effort is directed towards a metro-regional aerial transportation system being fully operational circa 2035.

II. Approach

To achieve the above-noted objectives there were three primary lines of investigation underpinning the technical approach for this study. First, NASA Design and Analysis of Rotorcraft (NDARC), a well-known NASA-developed rotorcraft conceptual design code, (see refs. 5-7), was enhanced to accommodate electric-propulsion-system modeling. This extended NDARC version was used to develop designs for a fleet of 6-, 15-, and 30-passenger helicopters with electric propulsion, known as Hoppers. The second major line of investigation was the development and analysis through simulation of a notional metropolitan aerial transit system based on the Hopper fleet—the primary emphasis being on the 30-passenger design—for three levels of assumed daily passenger ridership through the aerial transit system. A network topology software tool was used in conjunction with a custom-written discrete-event simulation tool called BaySim to support this particular focus of the study. The simulations also included a number of schedule optimizations to ensure that a given level of ridership could be accommodated with the minimum number of aircraft. The third and last line of investigation in the study focused on airspace interactions and the anticipated Air Traffic Management (ATM) system impact of a Hopper fleet concurrently sharing an already congested airspace filled with

conventional fixed-wing aircraft. This report documents the analysis and results for all three lines of investigation embodied in the study.

A. Hopper Aerial Vehicle Conceptual Design

The first line of investigation was to design aircraft at the conceptual level to produce a reasonably approximate performance model (size/weight of aircraft, number of passengers, takeoff/landing profiles, cruise speeds, power budget, etc.) that was then incorporated into a simulation of an aerial mass transportation network.

The initial vehicle conceptual design efforts focused on a small matrix of vehicles assessing combinations of takeoff and landing capabilities (STOL vs. VTOL) and the propulsion systems (conventional vs. electric). The STOL aircraft were designed so that they were able to clear a 50-foot obstacle within 1,500 feet of the beginning of the takeoff roll. These aircraft use standard fixed-wing-aircraft design capabilities embodied in the Program for Aircraft Synthesis Studies (PASS) (ref. 8) with the addition of a propulsion module that includes an advanced battery power source (parametrically defined using power volume and mass densities, maximum discharge rates, and temperature battery performance variations). The VTOL configurations are designed using the NDARC software (ref. 5) with some basic modifications for the electric aircraft versions. NDARC was augmented using the same battery and electric-propulsion module that was used for the STOL designs. For reasons of mission flexibility—and likely cost and availability of real estate for airport/vertiport siting—the aircraft conceptual design efforts ultimately concentrated almost exclusively on the VTOL designs: the STOL designs mainly served as a reference for the trade-offs in performance that resulted from the perceived requirement for a VTOL capability for the Hopper fleet.

Figure 2 illustrates the notional VTOL Hopper vehicles and vertiport stations considered for this study. As noted earlier, these vehicles—and turboshaft-driven baseline aircraft—were developed using the NDARC vehicle sizing software tool as a part of this study. The two smaller vehicles are single main rotor helicopters, whereas the larger vehicle is a tandem helicopter. More details regarding these vehicle designs are discussed later in this report.

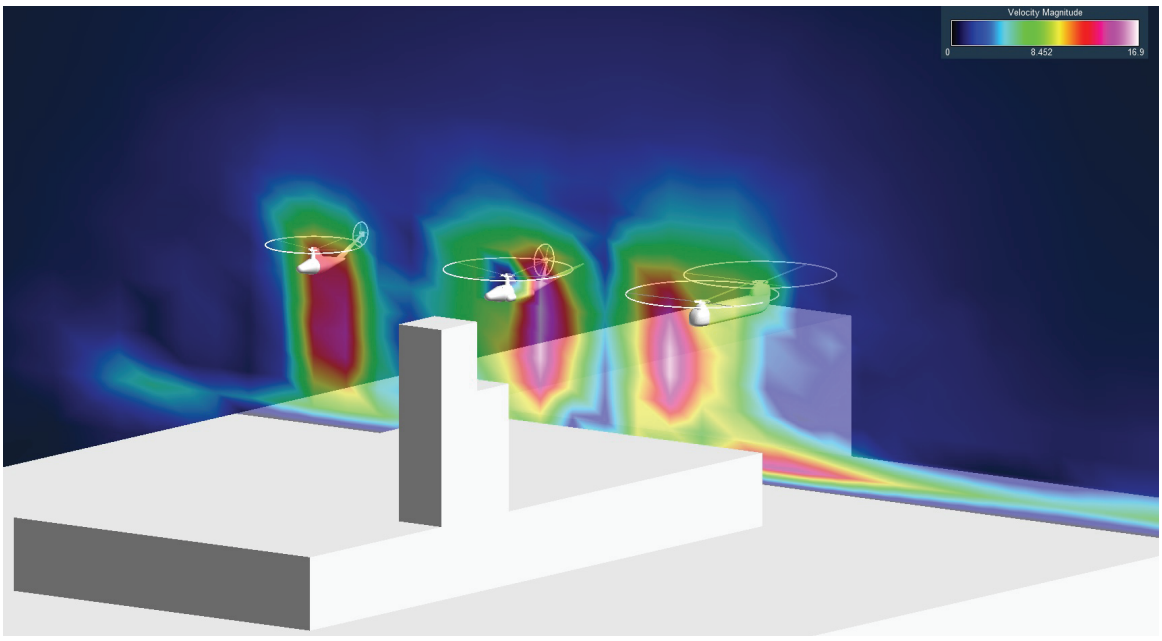

Figure 2. Hopper vehicles (6-, 15-, and 30-passenger) and vertiport station.

B. BaySim Hopper Network Simulation and Airspace Interactions

The second line of investigation in the study focused on the development of a simulation of the notional metropolitan-regional aerial transportation system in order to generate system performance data such as passenger throughput and point-to-point timing. A model network is defined in the San Francisco Bay Area as shown in figure 3. Figure 3 also illustrates (figure inset) a “flow corridor” concept in which Hopper vehicles might operate. Nodes of the network (stations) were selectively assigned (fig. 4). Five nodes from San Francisco to Gilroy are coincident with the CalTrain commuter line (ref. 9). Three nodes (San Francisco, Oakland, and Fremont) are coincident with the Bay Area Rapid Transit (BART) subway/light-rail system (ref. 10). This choice permits performance comparisons to the existing rail transportation system. A node in Santa Cruz was selected to determine the benefit of access to a coastal community separated from existing mass transportation systems by a mountain range. Because of the inherent nature of an air transportation system, all nodes can be connected point-to-point, regardless of intervening mountains or waterways. In the network, point-to-point distances range from 7 to 61 nautical miles (nm). The San Francisco Bay Area metroplex region was chosen for this study—not necessarily because it was the optimal location for a notional metro aerial transit system—but because it was anticipated to be a challenging analysis and simulation problem worthy of study and one well familiar to the authors.

At the overall system level it is desirable to design the best network possible, where measures of performance include: system-wide passenger throughput, environmental impact, impact on existing air traffic operations, Hopper air vehicle development, procurement and operating costs, and technology development required. This study focused on concept feasibility, not concept optimization. Economic considerations were not within the scope of the

Figure 3. Nodes of the model network (black dots) for an aerial mass transit system and (in the inset figure) a representative flow corridor between two of the nodes.

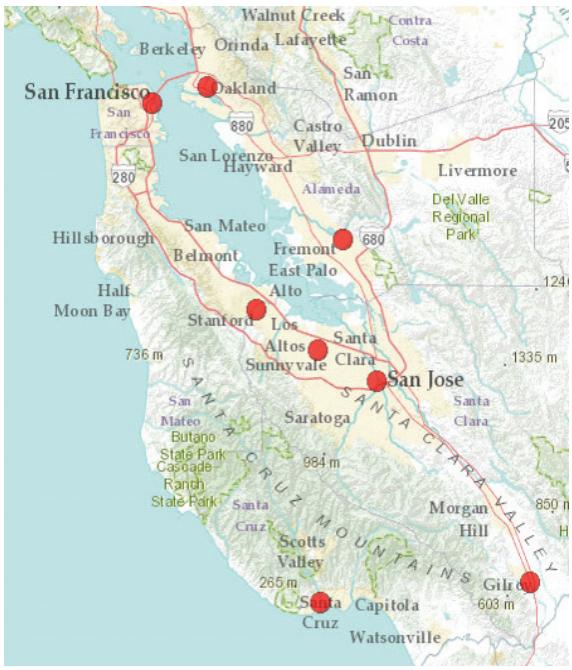

Fremont								
Gilroy	38.6							
Oakland	20.4	58.6						
Palo Alto	11.3	39.0	22.1					
San Francisco	23.8	60.9	6.0	22.7				
San Jose	14.1	25.3	33.4	14.3	35.6			
Santa Cruz	35.2	22.1	51.3	29.1	51.4	22.3		
Sunnyvale	11.0	31.6	27.9	7.5	29.5	6.8	24.4	

Station-to-Station Great Circle Distance, nm

Figure 4. Selected and analyzed Hopper aerial mass transit network and associated station-to-station distances.

current effort, although their importance in the ultimate realization of a feasible aerial mass transit system is acknowledged. To attempt to address the other measures of performance, a multidisciplinary analysis approach was taken. In the future, this initial analysis approach can and should be refined to enable an overall system optimization and design.

A variety of network topologies can be constructed to move passengers between stations, including point-to-point networks, hub-and-spoke systems, and linear (subway or rail-line-like) routes connecting adjacent stations (fig. 5). A point-to-point topology was selected for study. This network was assumed to maximize the benefit to an individual rider by providing timely service, while potentially stressing the air vehicle design as to meeting range requirements and the ability of the air traffic system to handle the added flights. The vertical expanse (upper and lower bounds of cruise altitude; e.g., fig. 3 inset) of the Hopper flow corridors explored in this study ranged from 1,000 to 5,000 feet above ground level (AGL). Nominal cruise altitude for the Hopper vehicles was a crucial consideration in examining potential loss-of-separation conflicts between the Hopper fleet and conventional fixed-wing aircraft traffic throughout the Bay Area, and encompassed the third line of investigation of this study.

To quantify the passenger throughput metrics, understand vehicle-sizing needs, and provide a system simulation upon which optimization can be performed, a daily passenger movement model was developed. BaySim is a discrete event simulation (DES) (ref. 11) that models passengers' behavior and their interaction with the Hopper air vehicles. The passenger agents in the model move through a series of discrete states over a 24-hour period, simulating their daily routine of arising, preparing for work, traveling to work, working, and returning home. The passengers' homes and worksites are distributed around the Bay Area population centers. Each passenger's movement through the transportation network is simulated. A set of queuing algorithms and flight generation heuristics are used by BaySim to generate Hopper flights between stations, based on the presence of individual passengers at each station. This results in a flight history logfile containing flight departure and arrival times, and the associated

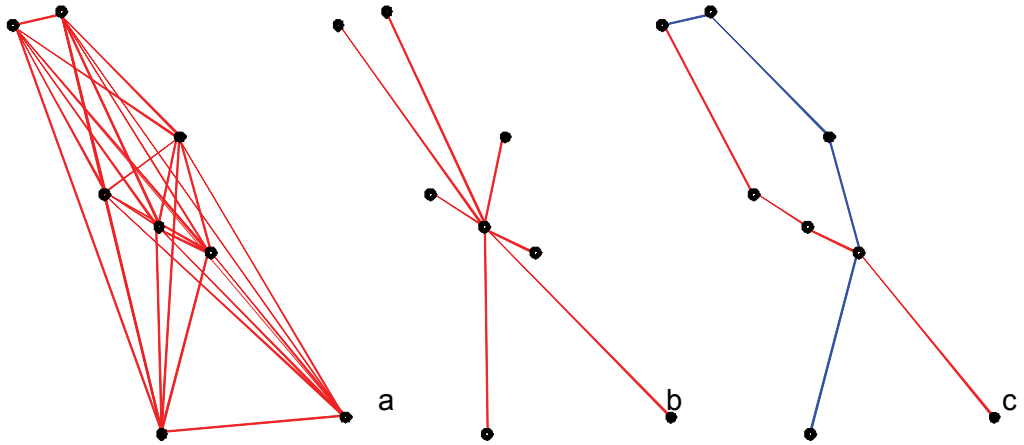

Figure 5. Potential Hopper network topologies for connecting stations: (a) point-to-point connections between Hopper stations; (b) (single) hub and spoke network; (c) a subway/ rail-line-like network

passenger load for the entire period of simulation. (Some of the detailed modeling features of the BaySim simulations, as well as key pseudocode, are discussed in the Appendix.) A daily Hopper flight schedule was derived from this data for subsequent input into fleet assignment optimization and air traffic simulation.

This study performed a daily movement simulation for three daily ridership levels of 5,000, 15,000, and 45,000 passengers to examine the impact of ridership variation. Based on the results of the movement simulation, three different Hopper air vehicle sizes of 6-, 15- and 30-passengers were selected to help support the target ridership levels. Using the flight schedule generated from BaySim as described above, and the selected air vehicle sizes, it was then possible to determine which Hopper should be used to perform each flight. This is known as the "fleet assignment problem" and is well known in the operations research literature (refs. 12,13). Here the objective was to assign a Hopper aircraft of a certain size to each flight—given the overall fleet composition—such that a cost function was minimized. A modified fleet assignment problem was subsequently constructed after the initial simulations and included the ability for Hoppers to perform repositioning flights between stations as necessary to serve the desired passenger schedule. The need to reposition is especially pronounced at the end of the day to get the vehicles to the appropriate stations for the following morning commute rush hour.

The study analyzed three different objective functions in the fleet assignment; minimum total cost, minimum number of aircraft, and minimum operating cost. The most realistic case is minimum total cost; accounting for the cost to both fly and own the Hoppers. The optimal result is a balance between the extra cost to own each aircraft and the additional flexibility gained by having each new aircraft. (Both the cost to own and the cost to fly the Hopper vehicles were estimated using the standard cost models incorporated in the NDARC conceptual design tool.) The second objective function represents another analysis case in which the total number of aircraft needed to support the ridership is minimized. For this objective function, all of the individual flight costs are equal to zero, and the ownership costs are equal to one. This objective examines the smallest feasible fleet and also represents the worst-case scenario for air traffic, as lots of repositioning flights will be used. The third objective function represents a case where the total direct operating costs are minimized, and the ownership costs are ignored. This is

expressed by setting the cost of vehicle ownership equal to zero. This is the best scenario for minimizing overall Hopper air traffic, as a minimal number of repositioning flights will be used, and it also gives an upper bound on the number of Hoppers required. These three objective functions were used in conjunction with network optimization tools to generate fleet size, mix, and overall projected traffic information that was then subsequently used in BaySim analysis.

System simulation tools were developed to determine the interplay between total patrons of the system, aircraft passenger count, fleet size, frequency of landings, passenger wait time, number of station stops, and point-to-point travel times. This information, as appropriate, was factored into the aircraft conceptual design process, as well as the assessment of the impact of Hopper operations on airspace traffic management. The key metric for Hopper airspace interactions was the estimation of the number of loss-of-separation events (between Hoppers and commercial air traffic) during a given time period. This airspace interaction assessment/ estimation was made by means of the well-known, NASA-developed Future ATM Concepts Evaluation Tool (FACET) software (ref. 14). This airspace interaction assessment was a crucial element of the overall study given the projected Hopper fleet size and number of daily operations.

In summary, figure 6 captures the general interactions between the disciplines and analysis tools applied in this study. Note that the figure 6 process was manual in nature and not automated. Further, figure 6 is somewhat idealized: though all disciplines/analysis tools were exercised during this study, only one “cycle” of the overall process was performed. A second round/cycle of analysis was not initiated because of time limitations during the study. In general, the figure 6 process was initiated with NDARC vehicle sizing analysis of a number of different vehicles and mission requirements. From NDARC, vehicle/mission performance numbers—vehicle cost estimates—were derived. This NDARC-derived information was then incorporated and used in the network topology (fleet assignment optimization) analysis. The resulting output from the network topology analysis was a definition of the fleet size required, as well as the daily number of commute flights and repositioning flights necessary, to support given different prescribed ridership levels and fleet mix. Subsequently, the NDARC vehicle performance information, and the fleet assignment optimization results, were used to establish the key input parameters for the BaySim Hopper simulation. The key result from the BaySim simulation was the spatiotemporal distribution of Hopper vehicles during a typical 24-hour commute period in the San Francisco Bay Area. In turn, the BaySim results were incorporated into a traffic density and loss-of-separation airspace analysis based on the use of the FACET software tool. Finally, the FACET results provided additional guidance as to refined vehicle mission requirements, particularly regarding cruise altitude and nominal range (qualitatively accounting for additional flight path circuitousness to attempt to minimize loss-of-separation events, wherein Hopper traffic interferes with commercial air traffic). If additional time had presented itself during the study, the new cruise altitudes and ranges defined by means of the FACET analysis would have been incorporated into a second generation of NDARC vehicle sizing. A more detailed discussion of the analysis and results from this study immediately follows.

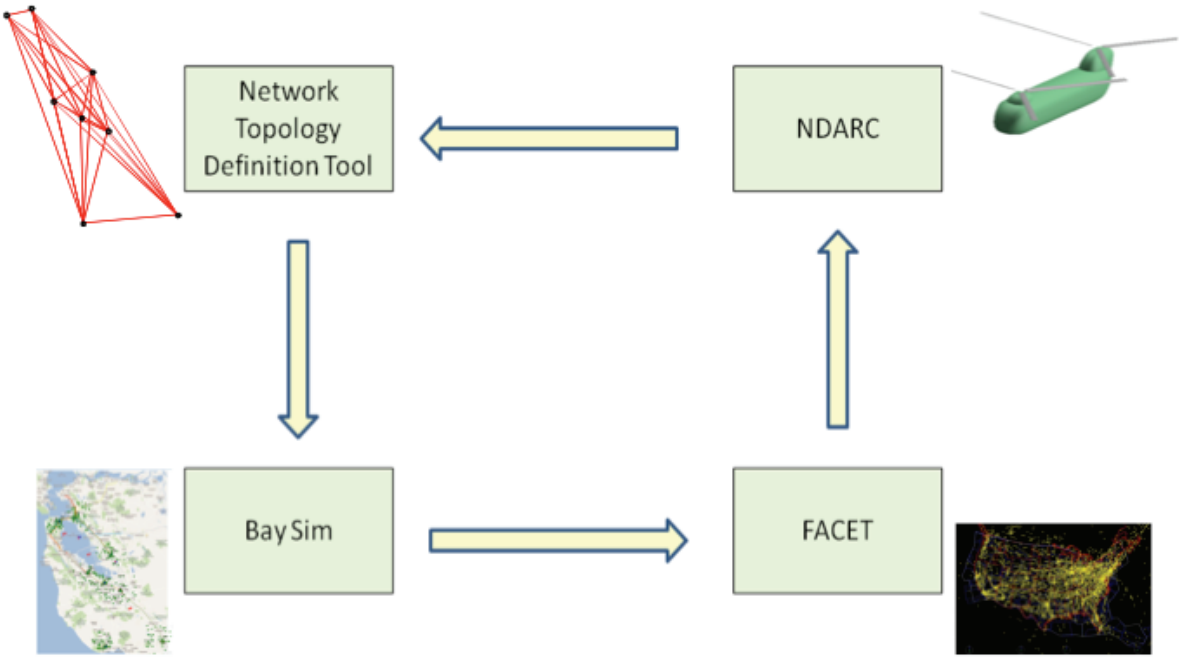

Figure 6. Interaction between the key disciplines and analysis tools used in this study.

III. Aerial Vehicle Design

A set of vehicles was designed in support of the aerial mass transit system modeling activities. As described above, three sizes were selected to provide a set of aircraft suitable for varying levels of passenger ridership/throughput in the mass transit system. Initial designs were completed using state-of-the-art turboshaft engine propulsion. These initial designs provided a point of departure for looking at potential alternative propulsion architectures. The goal of this alternative propulsion architecture trade study was to identify the level of technology required to enable a zero- or low-emissions rotorcraft for use in the aerial mass transit system. Accordingly, the following sections detail the assumptions and trades examined for an all-electric 30-passenger tandem helicopter design.

A. Electric-Propulsion Technology Survey

The aerial mass transit concept under study is intended to operate as a high-volume/high-frequency service, so its potential impact on carbon emissions and local air quality in the metropolitan area is a key environmental issue considered in the vehicle conceptual design. Among the current mass transit rail systems in the San Francisco Bay Area, BART is an electrified heavy rail system, and CalTrain presently uses diesel-electric locomotives to provide service. Given the extremely short vehicle range design requirements necessary to operate the Hopper network—and the desirability to be no more polluting than conventional rail transit systems—the conceptual design activity focused on alternative propulsion concepts. A 2030 time horizon was used in considering available technologies. The conceptual designs assumed technology improvements relative to current state-of-the-art rotorcraft consistent with those of the earlier NASA heavy-lift rotorcraft investigation for non-propulsion-related technologies/ vehicle systems (ref. 15). Particular focus was given to the conceptual design of an electric 30-passenger Hopper concept. This concept embodies the desired study attributes of being suitable for mass transit, environmentally friendly, and a potential target for focusing technology

investment to increase the role of aviation in intra-metropolitan transportation. While success with all-electric rotorcraft to date has been limited (e.g., ref. 16), continued improvements in energy storage densities and the relatively short-range requirements for a mass transit rotorcraft make the possibility of an all-electric rotorcraft intriguing for this application; figure 7 summarizes these trends (ref. 17).

A key challenge in moving away from current Kerosene-based propulsion systems is the very high specific energy of Jet A (11.95 kWh/kg) as compared to alternative forms of energy storage. This advantage in energy storage is partially offset by the relatively low overall thermal efficiency of turboshaft-driven rotor systems (~28%) as compared to electric drive schemes. While currently mass produced, Lithium-ion (Li-ion) battery systems are at about 0.180 kWh/kg specific energy; next generation Lithium-Sulfur (Li-S) battery chemistries achieving 0.350 kWh/kg have been demonstrated on QinetiQ's Zephyr HALE UAV (ref. 18). Further advances in Li-Polymer technologies show potential for achieving 0.650 kWh/kg (ref. 17) and beyond (refer again to figure 7). Battery technology is trending toward not only significantly higher specific energies, but also higher energy densities. These higher energy densities reduce the needed volumetric space for batteries in the airframe. A third area of concern in selecting battery technology is the specific power (kW/kg) of the technology. A trade-off in battery design must be made between specific power and specific energy. For Hopper air vehicle designs, the total required energy storage as compared to the peak power demand in hover results in a discharge rate that is 1.5C to 2C. Therefore, unlike hybrid systems where the battery capacity is relatively small and the discharge rates high, the necessary specific power of the battery system for an all-electric aircraft is less critical.

Conventionally powered rotorcraft enjoy not only an advantage in their specific energy, but also in the specific power of the turboshaft engine used to power the rotor. A modern turboshaft engine, like the GE CT7-8, has a specific power of 7.7 kW/kg (ref. 19). This compares favorably to a best-in-class 3.5 kW/kg for the Tesla Model R Roadster electric motor (ref. 20). The power required to hover a Hopper vehicle is significantly higher than that needed to propel a

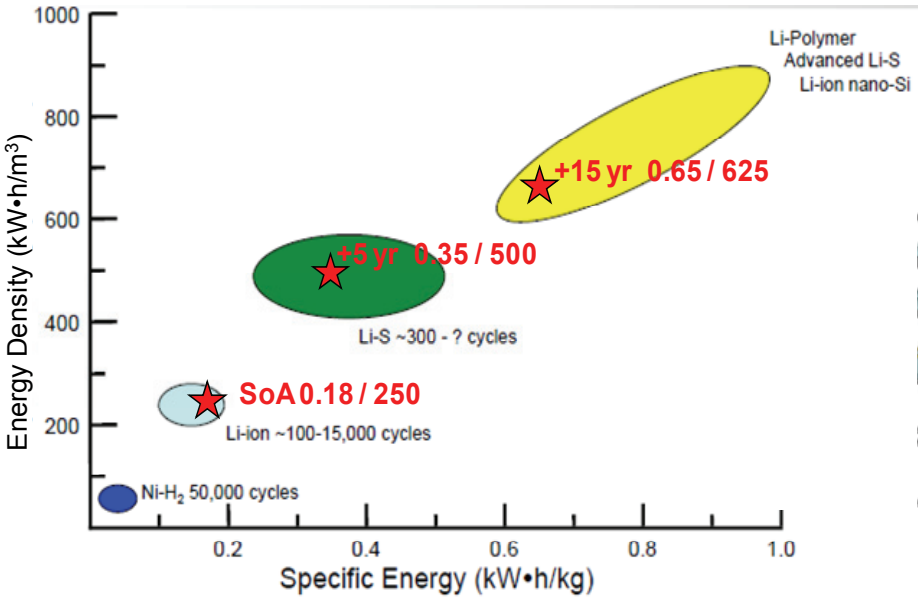

Figure 7. Battery-specific energy and density trends (ref. 17).

comparably sized (in terms of number of passengers) automobile, and it is anticipated that an electric Hopper concept will require a significantly more powerful motor than those currently being developed for automotive use. Using large industrial electric motors as a guide (fig. 8), a scaling law (Eq. 1) for state-of-the-art electric motors was developed:

$$W_{\text{motor}}(\text{lb}) = 1.96 \times P_{\text{motor}}^{0.8997}(\text{kW}). \tag{1}$$

Additional data points are shown on figure 8; in addition to large industrial electric motors, state-of-the-art automotive and axial-gap permanent magnet electric motors are shown by way of comparison. The specific power scaling indicated by this trend (Eq. 1) suggests that aviation electric-propulsion architecture trades might favor a system with fewer large motors as opposed to a large number of distributed small motors for driving the main rotor(s) of a rotary-wing vehicle. The state-of-the-art automotive motor data, though, also shows significant scatter compared to the trend line, suggesting that secondary factors other than total power output may be important. Improved scaling considering these factors is an item for future consideration. Considering the Tesla automotive motor as representative of good design, a 40-percent improvement relative to the state-of-the-art trend appears to be a reasonable assumption for the electric Hopper designs. Looking beyond continued improvements in AC induction and brushless DC motors, a study at NASA Glenn Research Center (ref. 21) of high-temperature superconducting motors suggests that even greater improvements in motor power-to-weight are possible. Glenn Research Center proposes the following scaling law (Eq. 2) for these motors (as also indicated by the purple line on figure 8):

$$W_{\text{motor}}(\text{lb}) = 2.28 \times P_{\text{motor}}^{0.6616}(\text{kW}) \tag{2}$$

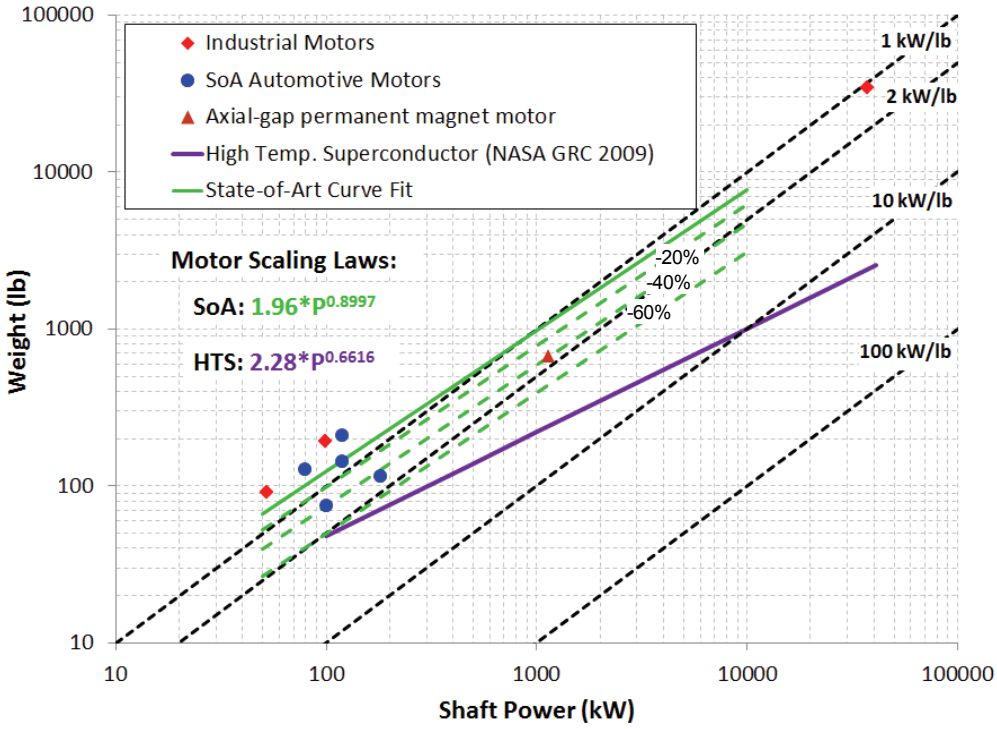

Figure 8. Electric motor scaling trends for both state-of-the-art automotive and industrial motors, and high-temperature superconductor motors (ref. 21).

While the proposed scaling of these motors favors high-power motors, a Hopper 1000 kW or higher class motor would be expected to have a specific power of 10.0 kW/kg and, given the relatively low technology readiness level (TRL) of high-temperature superconducting materials, makes achieving this motor performance goal high risk in the 2030 timeframe. As such, this level of technology was not considered further in the conceptual design activities of this study.

B. Propulsion Alternatives

In exploring low-emission alternatives to conventional Jet A powered turboshaft rotorcraft, a number of potential energy storage and power transfer alternatives exist. A subset of the possible combinations was considered qualitatively using the Pugh matrix shown in figure 9. It included two all-electric concepts, an alternative fuel, and hybrid concept.

These concepts were evaluated relative to the baseline in terms of performance, environmental factors, technology readiness level (TRL), cost, and operational considerations. These evaluations were made by means of subject matter expert input from study team members. All four alternatives are less attractive than the baseline Jet A/Turboshaft propulsion concept when considering the trade criteria on an unweighted basis. However, when one considers the potential importance of reducing greenhouse emissions and an associated rise in hydrocarbon-based energy prices, the advanced Lithium-polymer (Li-po) battery with AC motor configuration appears to be a potentially attractive alternative configuration that deserves further study.

An alternative fuel concept based on using ammonia (NH_3) as a fuel source was also evaluated in the Pugh matrix. Ammonia as a fuel has the potential advantages of an existing infrastructure for production, the ability to be combusted in existing turboshaft engines with minor modifications, and no carbon dioxide (CO_2) combustion by-products (ref. 22). Its primary disadvantages are the energy-intensive process presently used to create ammonia from natural gas, lower specific energy than Jet A, and overall toxicity.

++: significant improvement, +: improvement, 0: neutral, -: degraded, --: seriously degrade

		Energy Storage / Propulsion Alternatives				
Criteria		Jet A Turboshaft	Fuel Cell AC Motor	NH_3 Turboshaft	Adv. Li-po Battery AC Motor	Jet A / Li-ion Generator AC Motor
Energy Density	kJ/kg	BASELINE	--	-	-	-
Power Density	kW/kg		--	-	-	--
Emissions	kg/kW		++	+	++	+
TRL	-		--	0	--	0
Procurement Cost	$/shp		--	0	-	-
Energy Cost	$/kW		--	-	+	0
Complexity	-		-	0	+	-
Reliability	MTBF		+	0	+	0
Re-energize Rate	kW/min		-	0	--	0
Total		**0**	**-9**	**-2**	**-2**	**-4**

Figure 9. Pugh trade matrix of propulsion concepts considered for a Hopper design.

A hybrid drive system using a combination Li-ion battery storage system and Jet A fueled generator to drive an AC motor was also considered. Such a system would be able to take advantage of recharging opportunities at each station to store electric energy from clean generation sources in the Li-ion battery, reducing the use of Jet A. Battery capacity and weight would be less than that of a full electric system, but at the added cost of needing a generator and fuel system in parallel to the motor and battery electric system. This complexity would likely have a negative effect on system performance. It was also assumed that a hybrid system would tend to use lower tech (lower specific energy) Li-ion batteries to reduce technical risk and cost.

Fuel cell technology continues to mature, but generally lags battery technology in achieving higher specific energy densities (ref. 23). The reduction in moving parts and elimination of the high-temperature environment associated with gas turbines should result in favorable system reliability as the fuel cells mature. The future cost of hydrogen fuel remains an important unknown. Lower relative performance of the complete hydrogen storage and power system, coupled with increased complexity, development risk, and cost negatively impact this alternative.

An advanced Li-po battery coupled with high-performance AC motors offers potential for improved reliability and reduced greenhouse gas emissions, assuming clean sources of electric power. The relative simplicity of the battery, power control electronics, and electric motor should result in good reliability. One major challenge of battery-powered approaches is the relatively slow recharge rate, which will negatively affect turnaround time at each station. This can be overcome potentially by a battery quick-swap system with sufficient batteries appropriately pre-positioned at each aerial station (similar automotive automated battery quick-swap systems have been recently demonstrated; ref. 24).

Current Li-ion technology does not have a high enough specific energy to enable the desired electric Hoppers. Demand for high specific energy batteries in a variety of industries, however, has helped to ensure continued advancement in the technology, and significant improvements can be expected to continue in the next few decades. These advances make Li-po batteries a potentially acceptable alternative to Jet A, particularly for vehicles with lower design range and, possibly, lower passenger count. Note that a number of electric-propulsion options (including batteries, etc.) become potentially more attractive if economic incentives are introduced that help favor concepts that result in reduced emissions.

C. NDARC Conceptual Design Tool Extension to Accommodate Electric Propulsion

Using the NASA Design and Analysis of Rotorcraft (NDARC) tool (ref. 5), Hopper vehicle sizing was performed. A key advantage of NDARC is the ability to easily synthesize a broad spectrum of rotorcraft configurations using a library of preexisting components. NDARC is modular in nature and allows ready extension of the code to new components and analyses. As is typical of most conceptual design rotorcraft codes, NDARC combines parametric estimation of component weights, lower-order aerodynamic models, referred parameter engine modeling, and flight performance calculation routines to size a configuration. Sizing is the process whereby configuration design variables are adjusted until a specified set of mission and performance criteria are satisfied. Design optimization can be performed either by wrapping an optimizer algorithm around this sizing procedure, or in an ad-hoc manner where design parameters are systematically swept to establish sensitivities to guide designer selection of the

final design. This later approach, of sweeping parameters, was used in this study. (Rotor disk loading, required vehicle range, and battery-specific power were key parameters swept in the NDARC analysis to assess their impact on overall vehicle size and gross weight.)

For the electric Hopper configurations, it was necessary to extend the NDARC v1.6 propulsion module to include a model of a battery and motor. For this early conceptual design study, a simple model of each was used; only the peak power requirements, energy conversion efficiencies, and total energy required to complete the mission profile were considered. NDARC's basic approach of apportioning rotor and mechanical accessory power required to one or more turboshaft engines was followed for the apportionment of power to the electric motors.

Details of the mechanical transfer of power from the motors to the rotor system and mechanically driven accessories were simplified to consider just user-input power transfer efficiencies. Hopper is designed using the existing model in NDARC for mechanical transmission efficiency as a function of RPM and power. Efficiency for the motor in converting electric power to mechanical power is a user input, set to a constant 95 percent for this study. The motor is idealized to have constant efficiency regardless of power output; for a real motor, a significant reduction in efficiency can be expected when operating well off the design-point torque and shaft speed. The losses associated with the necessary power conversion and conditioning hardware is assumed to be 3 percent. This hardware is needed to convert the DC power supplied by the batteries to the appropriate AC signal for driving the motor at the desired speed. Finally, the batteries themselves have losses associated with the conversion from chemical to electric potential energy. This loss is taken as a constant 2 percent, regardless of power draw. The ratio of the power required at the rotor to the power required from the batteries (or other electric storage source) is then equal to the cumulative effect of the various component efficiencies (Eq. 3):[1]

$$\frac{0.746 \times \left(P_{\text{rotor}} + P_{\text{acc}}\right)}{P_{\text{batt}}} = \eta_{\text{batt}} \eta_{\text{motor}} \eta_{\text{pe}} \tag{3}$$

From Eq. 3, the necessary battery power can be determined at each flight condition or mission segment. Integration of the power required with time yields the necessary energy required for the design mission.

The simple power-law-scaling model developed in Eq. 1 is used to determine motor mass. For this study, details of the scaling of motor physical dimensions, as well as other intrinsic properties, were not considered (e.g., no slip speed, maximum torque, and no-load current values). A higher-fidelity propulsion analysis would require scaling laws for these properties as well. Battery weight, W_{batt}, is determined based on the installed battery capacity, E_{batt}, and an input battery specific energy, χ_{batt} (Eq. 4):

$$W_{\text{batt}} = E_{\text{batt}} / \chi_{\text{batt}} \tag{4}$$

Overall battery volume is also estimated based on an input specific energy. The necessary inputs and relations were added to NDARC by modification of the existing engine module, or "component," and an addition of a battery module/component, making it possible to model the motor-battery propulsion arrangement considered for this study.

[1] Note that the 0.747 constant in Eq. 3 is merely a conversion constant to convert from horsepower to kilowatts.

Beyond adding the inputs and performance models for the additional subsystem components described above, it was necessary to modify the mission performance and sizing solution procedures in NDARC for the electric Hopper. The typical NDARC mission performance solution procedure iterates until the fuel burned on the mission is equal to the fuel available at takeoff. Fuel burned is calculated by initially guessing a takeoff gross weight, and then sequentially evaluating each mission segment and decrementing the gross weight from the previous segment by the weight of the fuel burned on that segment. Mission total fuel burn is then used to update fuel available at takeoff and the corresponding takeoff gross weight. This forms a method of successive solutions that can be iterated on to convergence in most cases.

For the case of the electric Hopper aircraft where no fuel is burned, a different iteration scheme is required to calculate mission performance. An alternate formulation, based on comparing energy required to complete the mission to the energy available at takeoff, was used. This formulation has the advantage of being generalizable to many propulsion arrangements, including hybrid approaches where energy may come in multiple sources, to include both battery and liquid fuel. NDARC was therefore modified to calculate the energy required for each mission segment and to iterate until the energy available at takeoff equaled the energy required.

The sizing process in NDARC acts as an outer loop on the mission and flight performance routines. Similar to the mission performance solution procedure, a method of successive substitutions with relaxation is employed to converge critical design variables such as takeoff gross weight, rotor diameter, and installed power. For the electric Hopper, it was necessary to add battery capacity to this procedure. Convergence of the design is achieved when changes to gross weight, empty weight, and battery capacity are all within the specified tolerance for successive iterations.

D. Hopper VTOL Aircraft Configurations/Mission

Selection of three air vehicle sizes was completed based on initial passenger movement data from the 5k, 15k and 45k daily ridership simulations described in Section IV of this report. The 6- and 15-passenger Hoppers were designed as single main rotor helicopters, while the 30-passenger Hopper is a tandem helicopter configuration. (The single-main-rotor and tandem helicopter configurations were chosen as there is considerable design knowledge regarding their characteristics; this, accordingly, reduces the overall technical risk with respect to evaluating electric-propulsion versus conventional turboshaft propulsion performance.) All three aircraft were designed with relatively low disk loading (DL = 4.5 psf).[2] This low disk loading helps to reduce hover power loading as well as rotor wake hover-in-ground-effect (HIGE) outwash velocities. This was seen as particularly beneficial to the electric-powered Hopper, where specific power is significantly lower than for turboshaft aircraft, and hence will tend to favor lower power-to-weight ratios.

A simple mission profile (fig. 10) was developed for use in the sizing process. A design mission range of 65 nm was initially selected so that all stations on the network could be served point-to-point. It includes hover out of ground effect (HOGE) at the takeoff and landing, a small amount of start-up/warm-up time, and cruise at an altitude of 5,500 feet. This baseline cruise altitude was selected in recognition of a desire to reduce community noise impacts (ref. 26). Initial results from the air traffic conflict simulation indicate that 5,500-foot cruise altitude may not be the best system solution because of the increase in loss of separation events relative to a 3,000-foot cruise altitude. The vehicles that were designed during this effort, however, would also have the ability to complete their missions at the 3,000-foot cruise altitude.

[2] Typical helicopter disk loadings, DL = T/A, can range from 5 to 10 pounds per square foot (psf) (e.g., ref. 25).

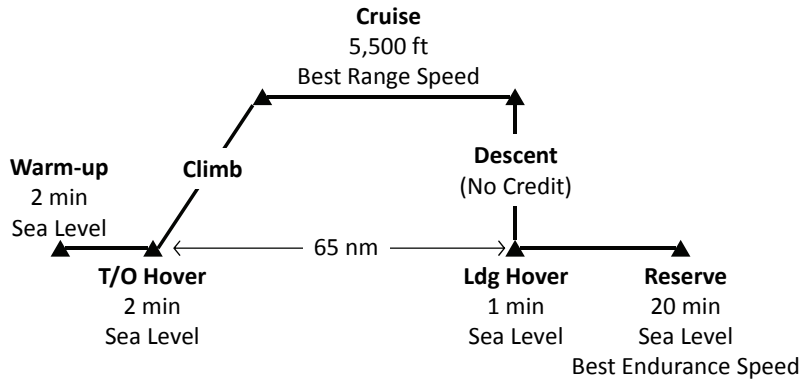

Figure 10. Hopper sizing mission profile.[3]

Additionally, rotor tip speed was kept low (650 feet per second) to reduce noise. Noise is one of several important considerations that are part of community acceptance of an aerial mass transit system. No further examination of noise was conducted in the present study, but it is an important consideration for future work. An additional 20 minutes of flight time at best endurance speed is assumed at the end of the mission profile. This reserve flight time is consistent with typical FAA minimums for daytime Visual Flight Rules (VFR) flight. On these types of short-haul missions, the reserve fuel/energy requirement can be a significant portion of the takeoff fuel/energy. Twenty minutes was felt to be sufficient to allow for the Hopper air vehicle to either hold for landing, avoid traffic conflicts, or divert to an alternate landing site and is consistent with previous studies (ref. 15).

For a high-tech aerial mass transit system, of which there are presently no operating examples, it was prudent to make a number of basic assumptions regarding acceptable design requirements that will ultimately be impacted by FAA regulation. Continued advances in cockpit automation should enable at least safe single-pilot operation. For a future mass transit system, consideration should also be made for potentially a fully automated system. Current commercial rotorcraft operations (e.g., ref. 27) require one-engine-inoperative (OEI) Category A hover performance at takeoff. This ensures that the aircraft can either safely return to the landing pad or has sufficient altitude to accelerate to a safe OEI forward flight speed. This requirement typically results in an increase in installed power beyond that required to HOGE. For this study, installed power sizing was done at a 3,000 feet/ISA+20°HOGE, under the assumption that a combination of descent energy management via advanced flight control, smart actuating landing gear, electric motor emergency torque capability, and overall reliability of the electric motor systems would bring the design to the same level of catastrophic hover risk level as is achieved by simply installing additional power to meet current OEI Category A requirements.

[3] Note that in figure 10 the “warm-up” terminology is primarily directed towards the turboshaft baseline aircraft, but it is still assumed to be necessary for vehicles with electric propulsion to undergo preflight system checkouts at low thrust/rpm prior to takeoff.

E. Hopper VTOL Aircraft Conceptual Design Results

All three aircraft classes were initially sized to the nominal 65-nm mission using a conventional turboshaft engine propulsion architecture. These aircraft provide a baseline for comparison when considering electric propulsion. Table 1 provides a summary of the three turboshaft-powered aircraft designs. The specific power of the propulsion system, including storage and power generation, is five times that of the specific power of current Li-ion batteries and highlights the challenge of designing an all-electric Hopper.

Figure 11 shows estimates of the takeoff weight fraction required for energy storage as a function of range. Estimates were made using the Breguet range equation and assuming vehicle L/De = 4.0.[4] This energy storage weight trend dominates electric Hopper designs.

Figure 11 also highlights the need to be extremely aggressive in reducing the empty weight fraction in all other areas of the vehicle design to provide a margin for growth in the battery weight fraction. Given that the smaller 6-passenger Hopper design tends to have a higher empty weight fraction because of unfavorable scaling down of items such as furnishings, cockpit, and vehicle management system, it will be harder to close (i.e., achieve NDARC convergence on vehicle weight/performance) on a feasible design for the smaller vehicle for the same level of battery technology and design mission range as compared to the larger 30-passenger Hopper.

The primary focus, though, was on the 30-passenger tandem electric Hopper because this vehicle size was found to be most relevant to the 45,000 daily ridership system and is, therefore, consistent with the vision of a high-capacity aerial mass transit system.

Table 1. Summary of Sizing Results for Turboshaft-Powered Hopper Designs

No. Passengers	–	6	15	30
Design Gross Weight	lb	5,421	9,770	20,313
Weight Empty	lb	3,547	5,763	12,364
Weight Empty Fraction	%	65	59	61
Prop. Grp + Fuel Weight	lb	988	1,674	3,723
Transmission Power	kW	486	843	1,896
Prop. Spec. Power	W/kg	1,083	1,108	1,120
Rotor Diameter	ft	39.2	52.6	53.6
Disk Loading	psf	4.5	4.5	4.5
Solidity (Geo)	–	0.0524	0.0524	0.0524
No. Blades	–	4	4	3
Blade AR	–	24.3	24.3	18.2
Tip Speed	fps	650	650	650

[4] An L/D_e of 4.0 is a typical value for a tandem helicopter (see e.g., ref. 28).

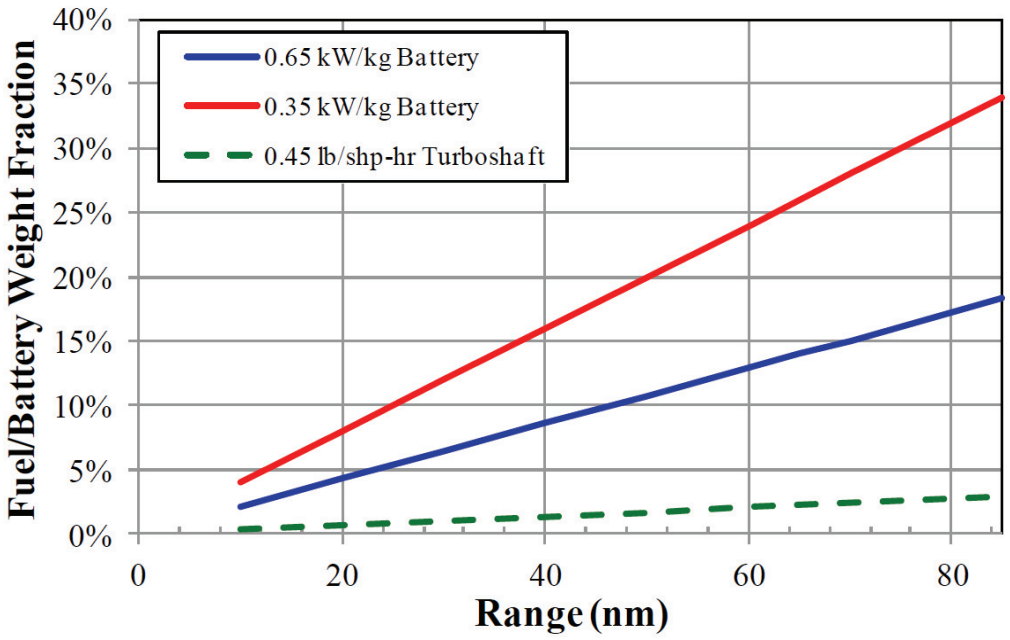

Figure 11. Impact of range on necessary stored energy required at takeoff for Jet A and Li-polymer.

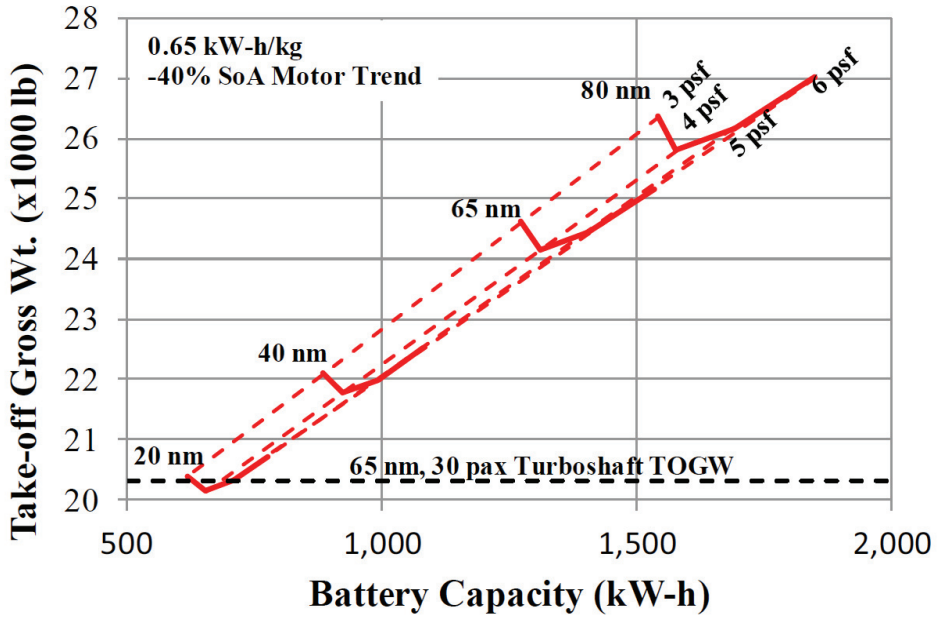

Figure 12. Variation in 30-passenger Hopper size with mission range and disk loading.

Figures 12 and 13 are NDARC sizing results for the 30-passenger electric tandem helicopter Hopper configuration. Figure 12 provides estimates of both required battery capacity (horizontal axis) and resultant vehicle takeoff gross weight (vertical axis) for a given combination of range (shown by red dashed lines running through demarked points of 20, 40, 65, and 80 nm) and disk loading (shown by red solid lines running through demarked points of 3, 4, 5, and 6 psf). Additionally, figure 12 provides by way of reference (a black dashed line) the takeoff gross

weight of a baseline, 65-nm-range, conventional turboshaft tandem helicopter design. As expected, for the electric Hopper designs, the greater the required range, the greater the necessary battery capacity and the heavier the vehicle. The results shown in figure 12 would suggest a secondary influence of disk loading on takeoff gross weight and battery capacity with DL = 4 psf being close to optimal for the configuration/mission studied, though more work would be required to confirm this result. Figure 12 shows that even with advanced Li-S battery technology (0.65 kW/kg) and relatively lightweight electric motors, the electric Hopper aircraft is significantly heavier than the conventional turboshaft design. A reduction in design range to an unconventional short distance (i.e., "extreme short-haul" missions as compared to the significantly greater ranges required for most other rotorcraft missions) is required to achieve comparable parity. The initial range of 65 nm was selected to ensure point-to-point service between any of the stations in the network. This initial sizing study indicates that moving to a centralized network, which would reduce the required aircraft range to 32 nm, would lead to an appreciable reduction in air vehicle size. An additional consideration in the design range not yet fully explored is the potential need for non-direct routing between stations to integrate with the existing air traffic flows in the Bay Area. This is an excellent example of how a multidisciplinary approach to the overall mass transit system optimization can open up needed design space to achieve a better result.

The strong impact that improving battery-specific energy (going from 0.18 to 0.35, and finally to 0.65 kW-h/kg) has on electric Hopper size and viable mission range is seen in figure 13. Figure 13 provides estimates of both required battery capacity (horizontal axis) and resultant vehicle empty weight (vertical axis) for a given combination of range (shown by red dashed lines for 20, 40, and 65 nm) and battery-specific energies (shown by red solid lines for 0.35 and 0.65 kW-h/kg). For state-of-the-art 0.180 kW-h/kg battery-specific energy, the aircraft is intolerably large at even extremely short mission ranges (in this case restricted to a single reference point for vehicle range, 10 nm, as illustrated by the small triangle shown on figure 13).

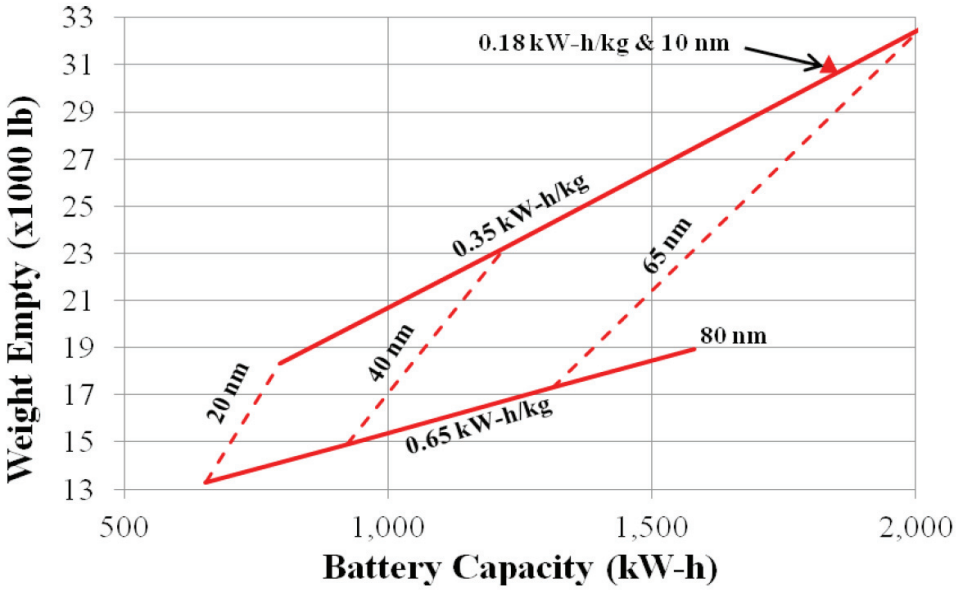

Figure 13. Impact of battery-specific energy on electric Hopper size and viable mission range.

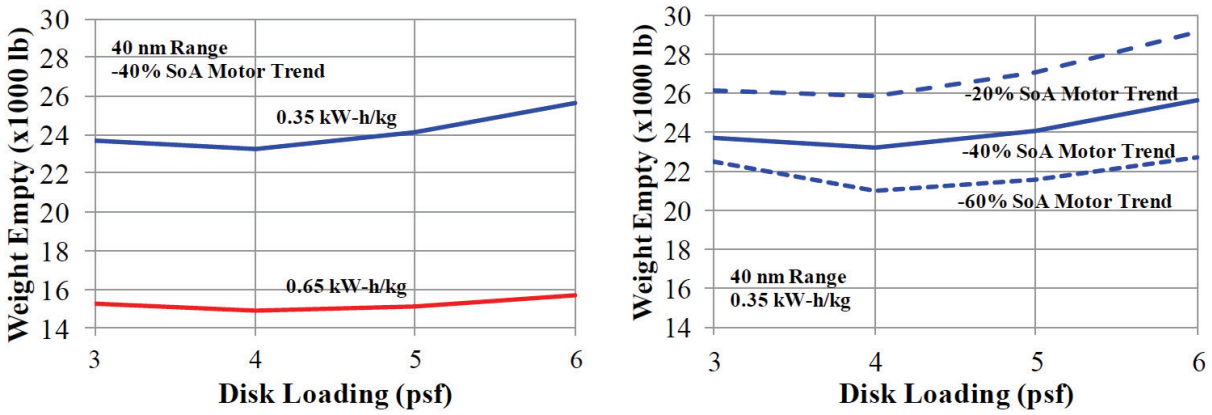

Figure 14. Impact of two levels of battery-specific energy and three motor weight trend levels on vehicle empty weight.

A parametric sweep of rotor disk loading (fig. 14a-b) for two levels of battery-specific energy and three motor weight trend levels shows that the optimum disk loading remains relatively constant, at approximately 4 psf, regardless of the assumed technology level of the batteries or electric motors. The more pronounced influence of battery-specific energy on vehicle empty weight as compared to motor weight reductions is also apparent in figure 14a-b. All NDARC results for figure 14a-b are for a design range of 40 nm.

Table 2 summarizes three 30-passenger electric Hopper designs (for different combinations of design ranges and assumed battery-specific energies) as compared to a single baseline turboshaft design. The initial results indicate a desirability to reduce the design range and the importance of higher specific energy battery technology. To significantly reduce the Hopper vehicle design range, though, requires a reexamination of the Hopper network topology; both design problems (vehicle and network) are coupled together. Further, because of the cascading effect that increased battery mass has on overall vehicles size, the results also indicate that paying more in dollars per kilowatt-hour for a higher specific energy battery system is likely preferred. It is also clear from the initial results that how the long-term (circa 2030, as posited by this study) economics play out between electricity and hydrocarbon-based fuels will be important. The initial price premium likely required for an all-electric vehicle would have to be recouped through lower energy costs associated with operations. In addition, the potential for higher reliability with the electric propulsion system could be attractive in the context of a high-frequency mass transit system.

Figure 15 illustrates the relative size of the four 30-passenger tandem helicopter designs (one turboshaft baseline design and three different electric designs). Additionally, the size of the 30-passenger Hopper vehicle is shown in relation to arguably the first manned electric helicopter. This small coaxial helicopter was developed and flown (in HIGE) by Pascal Chretien of France on August 12, 2011. The takeoff gross weight (TOGW) of the vehicle was 545 lb, the electric motor was nominally 32 kW, and the custom Li-ion battery was nominally rated at 9.2 kW-h (ref. 16). Showing the vastly greater size of the electric Hopper vehicle compared to the Chretien coaxial helicopter highlights the technology hurdles that have to be overcome to scale up VTOL vehicles to achieve Hopper-like missions.

Table 2. Comparison of 30-Passenger Electric Hopper Designs With Baseline Turboshaft Concept

		TS	Electric		
No. Passengers	–	30	30	30	30
Design Range	nm	65	65	40	40
Stored Spec. Energy	kW-h/kg	12.0	0.650	0.350	0.650
Design Gross Weight	lb	20,313	24,148	30,096	21,768
Weight Empty (Less Battery)	lb	12,364	12,382	14,986	11,794
Weight Empty Fraction	%	61	51	50	54
Energy Storage Fraction	%	5	20	27	14
Prop. Grp + Energy Storage Wt	lb	3,723	6,906	10,660	5,386
Maximum Rotor Power	kW	1,896	1,834	2,227	1,677
Prop. Grp Spec. Power	W/kg	231	121	95	142
Take-off Energy	kW-h	–	1,311	2,009	923
Conv Efficiency	%	28.1	90.3	90.3	90.3
Storage Volume	gal.	858	554	645	390
Rotor Diameter	ft	53.6	62.0	69.2	58.9
Solidity (Geo)	–	0.0524	0.0465	0.0465	0.0465
No. Blades	–	3	3	3	3
Blade AR	–	18.2	20.5	20.5	20.5
Tip Speed	fps	650	650	650	650

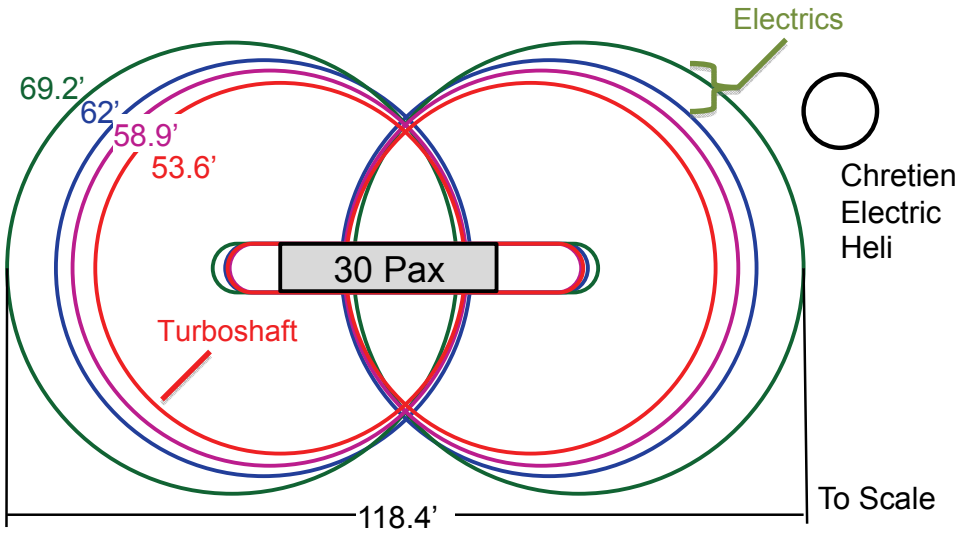

Figure 15. Relative planform size of vehicles listed in table 2.

Figure 16 shows the estimated energy expenditure breakdown of one of the 30-passenger Hopper variants studied (the 62-foot-diameter rotor electric vehicle designed to the 65 nm range and an assumed 0.65 kW-h/kg battery capacity; leftmost electric vehicle column in table 2). One of the key considerations of the energy budget, the size of the reserve provided for in the vehicle design, is readily seen in figure 16. As noted earlier, a 20-minute reserve has been assumed; this reserve represents 27 percent of the energy budget.

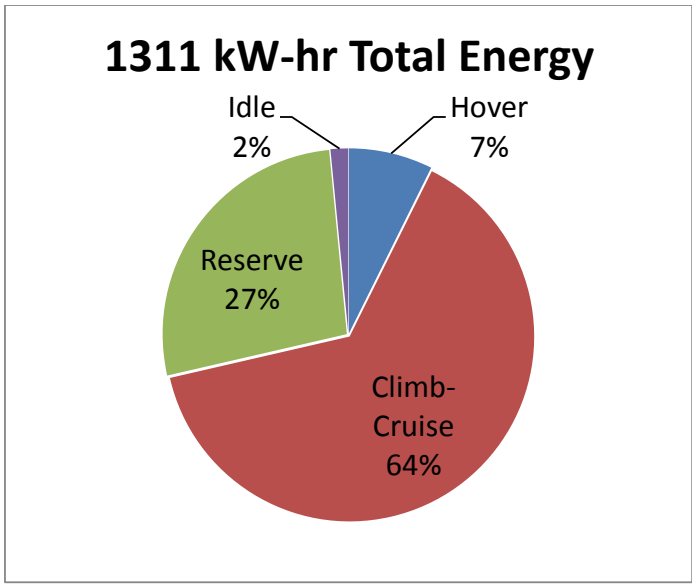

Figure 16. Energy expenditure breakdown for 62-ft-diameter 30-PX Hopper electric tandem helicopter.

IV. Metropolitan-Regional Aerial Transit System Simulation

A. Estimating Ridership Levels

It was assumed to be too challenging, given the overall scope of the study effort, to develop a demand model for a Hopper fleet comprised of wholly new aircraft and an associated novel CONOPS, circa 2035. Instead, gross ridership levels were developed using some general Bay Area public transit statistics. The BART system supports approximately 370,000 riders on weekdays (ref. 10), while the number of Bay Area "tech industry" workers in 2008 was reported to be approximately 386,000 (ref. 29). The peninsula railroad service (CalTrain) between San Jose and San Francisco serves over 40,000 passengers per day (ref. 30), and this level of ridership (spread out across the entire Bay Area) was deemed by the team to be a worthy end goal for Hopper passenger service. In lieu of a Hopper demand model, the team used the above noted Bay Area public transportation ridership information to bracket/benchmark the notional Hopper ridership levels; the study team consensus being that Hopper ridership levels might approach, but were unlikely to exceed, reported Caltrain ridership levels. With these considerations, three ridership levels of 5,000, 15,000, and 45,000 passengers were chosen for the study to explore Hopper operational considerations.

In addition to establishing the assumed Hopper ridership levels, the workdays for passengers were distributed such that 65 percent of a population would work a "day" shift that started between 4:00 AM and 10:00 AM, lasting 7 to 9 hours. Twenty percent of the population were assigned to a "swing" shift, which started between 1:00 PM and 6:00 PM, and also lasted between 7 to 9 hours. Five percent of the ridership population were placed on a "night" shift that started between 9:00 AM and 2:00 AM, and lasted between 7 to 9 hours. The starting times for the remaining 10 percent of the population were then randomly distributed between 8:00 AM and 3:00 PM, with workdays lasting between 4 to 5 hours. These workday start times and

durations were not based on any demographic data, but were chosen through consensus among the study team members.

The above ridership assumptions were incorporated into the BaySim Hopper network simulation.

B. BaySim Simulation Overview

The computer simulation of individual human behavior is (and will always be) an imperfect science. An individual's choices and daily behaviors are often complex, usually irregular, and sometimes illogical. But when a large group of individuals is aggregated to form a population, the behavior of that population can be conveniently modeled by statistical averaging over the individuals. This process is commonly referred to as microsimulation. A common example of a microsimulation is the study of highway traffic patterns, with gross characteristics of the traffic flow extracted from the statistical aggregation of individual autos (e.g., ref. 31). Inside a microsimulation, the variation in the behaviors of individuals is commonly modeled with a relatively small set of stochastic mathematical functions that create appropriately bounded and distributed randomness in individuals (usually subject to Gaussian-like distributions). This is especially true for actions that all individuals perform with some amount of regularity. In the Hopper transportation model, it is assumed that during the work week, the demand for transportation arises from the need of individuals to transit from home to workplace and back again, with this cycle repeating for each individual once every 24 hours. Once the rules that govern daily passenger decisions and behaviors are described in software, they become the framework for a discrete event simulation (DES) of the demand for transportation in an extended metropolitan area. In this case, the daily demands on a metro-regional transportation network are derived from analysis of the aggregate behavior of passengers as they move through the transportation network. This demand for transportation is provided as input to a fleet optimization process (described in detail later in the report), which is used to determine the total number of vehicles required to satisfy the transportation demand while minimizing the overall cost of transportation. Note that this approach to transportation network analysis does not start with either a predefined vehicle concept or a preset schedule. Instead, every attempt has been made to develop a bottom-up demand model from the two most basic elements: realistic passenger behaviors and the geographic characteristics of home, air terminals, and workplace. Somewhat surprisingly, vehicles in the BaySim DES need not be initially described beyond the most basic performance characteristics of capacity (passenger count) and speed.

BaySim, the custom DES simulation tool that was developed for this study, has several noteworthy features, including the modeling of individual passengers and aircraft. Each passenger transitions through nine different states during a 24-hour day, and each aircraft transitions through four states during each flight (refer to the Appendix for a detailed description of the passenger/aircraft states). Transitions between the passenger/aircraft states are governed by a finite state machine (e.g., ref. 32) using combinations of time of day, random numbers, and queuing/scheduling strategies. Currently, the population is segregated into three primary shifts (day, evening, and night), and geographically distributed around the major population centers of the Bay Area. On-screen graphics provide animations of both passenger and aircraft states and motions, and real-time plots of network statistics (delays times, queue lengths, departure and arrival counts, etc.) are available. A screen capture from the BaySim DES is shown in figure 17. The left pane of the image provides a graphical display of the status of all population members. Solid green dots represent individuals who are at their homes or traveling along the surface toward their home air terminal. Red triangles indicate passengers who are currently grouped together aboard an aircraft and flying toward their workplace air

terminal. Black squares show individuals moving along the surface from their workplace air terminals towards their worksites. Blue dots show workers who have finished their workday and are returning along the surface to their worksite air terminal. Blue triangles represent passengers who are aboard return flights that will take them to their home air terminal, and green open dots show individuals who have arrived back at their home air terminal and are moving along the surface to return home at the end of their workday.

Where possible, stations were located at or very near existing surface transit hubs (Caltrain or BART terminals). This assured that passengers would have only a very short walk to reach train or bus services. Co-locating Hopper nodes with surface transit nodes also used existing parking facilities for those passengers entering or exiting the system by bus or automobile. Businesses and home sites were randomly distributed throughout the Bay Area, with additional concentrations in the cities of San Francisco, Oakland, and San Jose, and the outlying communities of Gilroy and Santa Cruz. Group consensus and experience with the Bay Area drove the initial distributions, not specific population or census data. This was considered to be appropriate for this effort, which was intended to provide only initial estimates of the number of Hopper aircraft and flight operations required to serve populations of various sizes.

Note that adapting the BaySim DES to other geographical areas of interest and/or station network topologies should be straightforward, but would require geographic information about home and worksite locations as input. Aircraft speed, capacity, and minimum required load factors are all available as inputs, allowing aircraft of various capacities to be simulated.

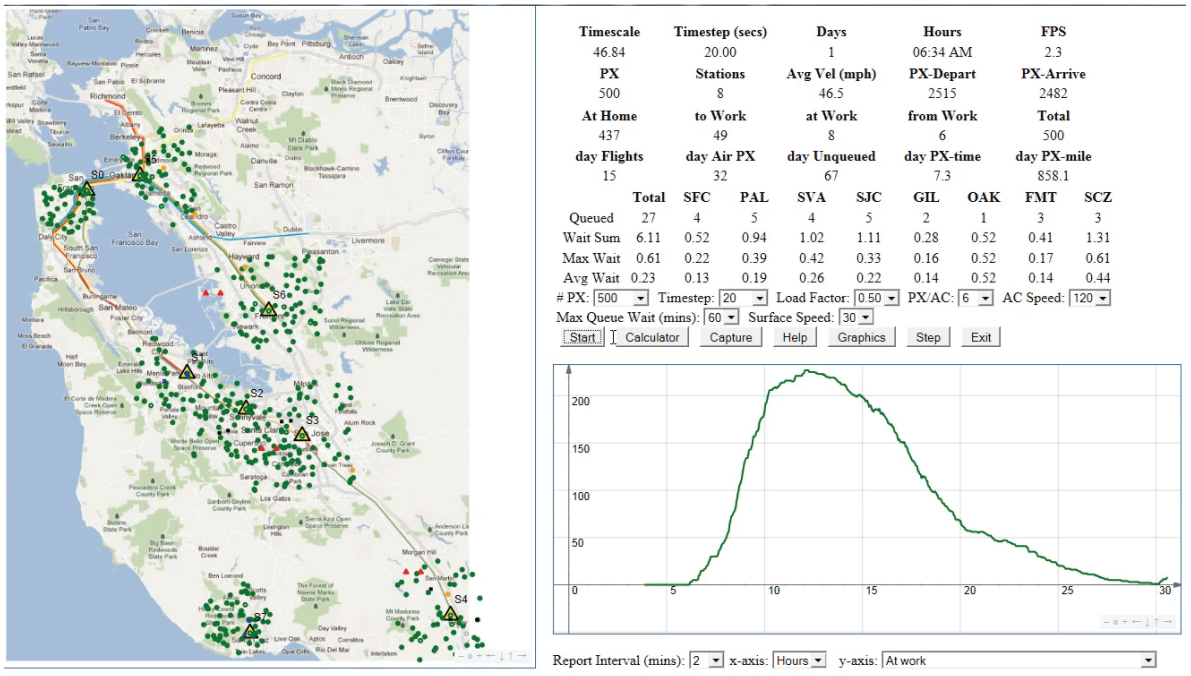

Figure 17. Screen capture of BaySim DES animation.

C. BaySim Hopper Results

Initial BaySim simulation results for the Hopper aerial transit system are presented below for the three assumed ridership levels: 5,000, 15,000, and 45,000 passengers per day. No attempt was made to characterize total ridership level in terms of passenger demand (taking into account ticket price estimates and other factors such as point-to-point travel speed/convenience); such an effort was considered to be too speculative and out of scope with respect to the primary objectives of the study.

Figures 18 and 19 are representative BaySim simulation time history results. In both figures, the passenger states are captured in an hour-by-hour basis. Figure 18 shows the time history of the number of passengers (passenger count) in various passenger states. Figure 19 shows the time history of the number of passengers traveling to and from work. In particular, the 24-hour cycle repeatability as evidenced in these two figures is a good indicator of the stability/convergence of the BaySim simulations.

BaySim analysis for this initial study yielded the following insights: average trip length was 28 statute miles; average time in air per flight was 14 minutes; at the maximum assumed ridership level of 45,000 passengers per day, 1,712 operations per day per station (assuming 8 stations) would be carried out. By way of comparison, San Francisco International Airport (SFO) currently supports approximately 1,100 operations per day (arrivals and departures) for 112,000 passengers per day. Table 3 provides additional details for all assumed ridership levels studied.

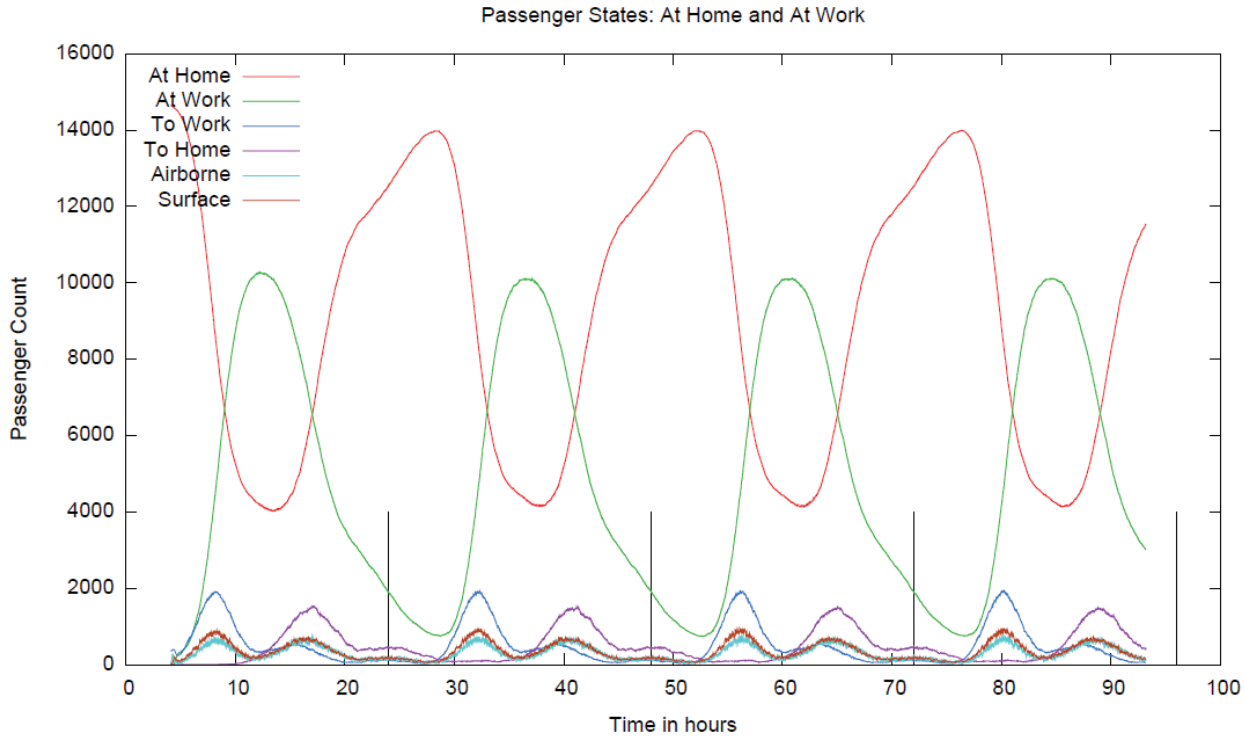

Figure 18. BaySim passenger count estimates of passengers at home and at work.

Table 3. BaySim Results Summary

Population	Minutes Between Departures (MBD)	Daily Flights (Minutes)	Simultaneous Flights (Maximum)	Maximum Preflight Delay (Minutes)	Passenger Miles (Daily)
5K	3	1,940	40	10	270K
15K	3	3,140	47	15	834K
15K	1.5	4,010	71	6	836K
45K	1.5	6,250	84	13	2,494K
45K	1	6,850	100	3.5	2,494K

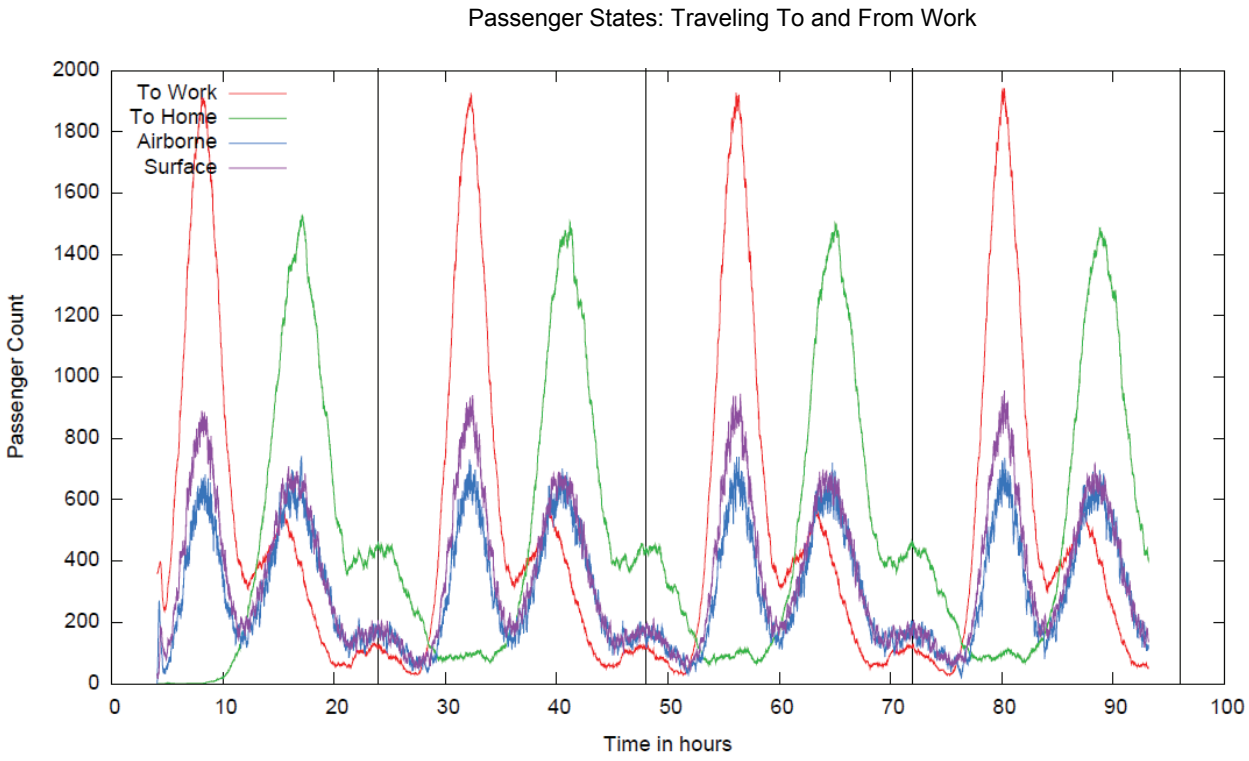

Figure 19. BaySim passenger count estimates traveling to and from work.

Numerous Hopper network metrics and their estimates were made possible with the BaySim simulation. For example, initial BaySim results allowed the following estimates to be made: 1) at the 5,000-per-day passenger level, the estimated energy expenditure for the aerial transit network was 6,700 BTU/PX-mile, with an average number of passengers per vehicle of 5.1 PX/vehicle; 2) at the 15,000-per-day passenger level, the energy expenditure was estimated at 4,530 BTU/PX-mile, with an average of 7.5 PX/vehicle; and 3) at the 45,000-per-day passenger level, the energy expenditure estimate was 2,570 BTU/PX-mile, with 13.2 PX/vehicle.

D. Hopper Fleet Sizing Strategy

One of the major outputs from BaySim is a schedule of flights and a number of passengers flying on each flight; this schedule of flights is implicit in the representative passenger state results presented in figures 18 and 19 and the analysis summary in table 3. This schedule was subsequently used to determine what size (in terms of number of passengers) Hopper vehicle should fly each flight. This fleet assignment problem is well known in the Operations Research literature (e.g., refs. 33,34). In the fleet assignment problem, the goal is to assign one member of the fleet (Hopper size) to fly each flight in the schedule such that cost (or some other efficiency measure such as fleet size) is minimized. The fleet assignment problem is shown in Eq. 5. Specifically, the schedule consists of a set of flights, F, that fly between the N stations. Each flight has a demand, p_f, (i.e., the number of people who would like to be on flight f) that must be serviced. There are a set of aircraft types, K, that each have a cost, $C_{f,k}$, to fly each flight, a cost of W_k to own (which includes both procurement and maintenance costs), and a capacity of b_k passengers. The optimization is over binary decision variables, $y_{f,k}$, which equal one if fleet member k is flying flight f, and zero otherwise.

The objective is to minimize the total sum of costs, subject to a guarantee that each flight in the schedule will be flown. Of course, for a flight to be flown with a certain fleet, an aircraft of that type must be present at the station when needed. A set of variables, $G_{n,k,t}$, is used to represent the number of aircraft, in fleet k, on the ground at station n, at time t. In the fleet assignment problem, time is not measured in seconds, but rather by the number of flights that have either taken off or landed at that station. As a result, each station has its own "clock," where time 0 is the beginning of the day, time 1 is after the first arrival or departure, time 2 is after the second arrival or departure, etc., and time T is after the last takeoff or departure of the day for that particular station.

A set of constants, $S_{n,t}$, mark the type of event, with a value of one when the event at time t is an arrival, and a value of negative one when the event is a departure. Lastly, to ensure that the schedule can be flown more than once (on successive days), an additional constraint is added; it requires that the number of Hoppers of each type on the ground at the end of the day be equal to the number of Hoppers that started on the ground.

A modified version of the fleet assignment problem is being employed that allows for the full cost of these repositioning flights H to be fully accounted for. These are especially useful at the end of the day to meet the periodicity constraint, and during rush hour, when, for example, there may be more demand going into San Francisco than out of it. The repositioning flight variables are represented by $z_{h,k}$, which are binary variables that equal one if the flight is flown and zero otherwise. Each repositioning flight has a cost of $D_{h,k}$ to fly, but unlike flights in the true schedule, there is no requirement that specific repositioning flights be flown.

$$
\begin{gathered}
Minimize: \\
\sum_{k \in K}\left(\sum_{f \in F} C_{f,k} y_{f,k} + \sum_{h \in H} D_{h,k} z_{h,k} + \sum_{n \in N} W_k G_{n,k,0}\right) \\
Subject\ to: \\
\sum_{k \in K} y_{f,k} = 1 \quad \forall f \in F \quad (All\ scheduled\ flights\ flown) \\
\sum_{k \in K} b_k y_{f,k} \geq p_f \quad \forall f \in F\ (Flight\ demand\ met) \\
G_{n,k,t-1} + \sum_{f \in F} S_{n,t} y_{f,k} = G_{n,k,t} \quad \forall n \in N, t \in T, k \in K\ \ (Aircraft\ tail\ number\ continuity) \\
G_{n,k,t} \geq 0 \quad \forall n \in N, t \in T, k \in K\ \ (Non-negative\ number\ of\ aircraft) \\
G_{n,k,0} = G_{n,k,T}\ \ (Periodicity) \\
y_{f,k} = \{0,1\} \quad \forall f \in F, k \in K \\
z_{h,k} = \{0,1\} \quad \forall h \in H, k \in K.
\end{gathered}
\tag{5}
$$

Three different objective functions were analyzed using the optimization methodology centered around Eq. 5: minimum total cost, minimum number of aircraft needed in the fleet, and minimum operating cost. The most realistic case is minimum total cost accounting for both the cost to fly and the cost to own the Hoppers in the fleet. The optimal result is a balance between the extra cost to own each aircraft and the additional flexibility gained by having each new aircraft. The second objective function is a case in which the total number of aircraft needed is minimized. For this objective function, all of the flight costs ($C_{f,k}$, $D_{h,k}$) are set equal to zero, and the ownership costs (W_k) are equal to one (so that the actual cost computed by the optimization equals the total number of vehicles in the fleet). This objective examines the smallest feasible fleet, and also represents the worst-case scenario for air traffic, as lots of repositioning flights will be used. The third objective function is also a case where the total direct operating costs are minimized and the ownership costs are ignored. This is expressed by setting all of the ownership costs (W_k) equal to zero. This is the best scenario for air traffic, as a minimal number of repositioning flights will be used, and it also gives an upper bound on the number of desired Hoppers.

Each of the three objective functions was optimized for the 5,000-, 25,000-, and 45,000-passenger BaySim schedules. The optimization was done using the Gurobi mixed-integer programming optimization suite, a software tool (ref. 35) designed specifically for mixed integer linear problems. The results of all optimizations are summarized in table 4.

There appears to be a distinct tradeoff between the number of repositioning flights and the number of Hoppers owned. The two cases are quite different; the minimum fleet size is much smaller and has many more repositioning flights than the minimum direct operating cost case. However, the minimum total cost solution has only a few more Hoppers than the lowest possible, and only a few more repositioning flights than the smallest possible. Not surprisingly, as the number of passengers grows, the percentage of the fleet that is 30-passenger Hoppers grows. For the 5,000-passenger case, no 30-passenger Hoppers are needed, while for the 45,000-passenger case, the fleet is almost entirely 30-passenger Hoppers. Finally, as the number of passengers grows, the maximum number of Hoppers on the ground at a time also grows. While this was not a part of the objective function (and so no firm conclusions can be drawn), the results suggest that vertiport station space may be an issue, and that further work should take into account station infrastructure costs.

Table 4. Aerial Transit System Network Optimization and Hopper Fleet Assignment

No. of Pax	Opt. Target	No. Flights		No. Aircraft				Max A/C at SF Sta.
		Reposition	Total	6 Pax	15 Pax	30 Pax	Total	
5k	DOC	17	1,830	43	73	0	116	14
	Total LCC	36	1,866	29	26	0	55	7
	Fleet Size	1,804	3,634	–	–	–	46	6
15k	DOC	18	3,155	83	64	57	205	25
	Total LCC	59	3,214	17	3	37	57	7
	Fleet Size	1,959	5,114	–	–	–	54	6
45k	DOC	14	6,825	32	51	125	208	51
	Total LCC	35	6,860	11	12	106	129	24
	Fleet Size	3,689	10,514	–	–	–	109	18

(DOC = Direct Operating Cost optimization; Total LCC = Total Life Cycle Cost; Fleet Size = minimum fleet size)

V. Airspace Interactions

This section describes the primary simulation environment that was used to explore the interactions between the Hopper fleet and the existing air traffic. Additionally, the key metric that was used to quantify these interactions is introduced and results of fast-time simulations experiments are discussed.

A. Airspace Simulation Environment

NASA's Future ATM Concepts Evaluation Tool (FACET) (ref. 14) was the primary simulation system used to investigate the potential interactions between the Hopper fleet and the surrounding traffic in the Northern California Terminal Radar Approach Control (NCT)—also known as the NorCal TRACON—facility. FACET is a flexible, national-level ATM simulation system that has been used extensively for exploration, development, and evaluation of advanced ATM concepts. The architecture of FACET strikes an appropriate balance between fidelity and flexibility, which enables it to model the trajectories of over 6,000 flights at any instant in time on a standard commercial off-the-shelf laptop system. An image showing the primary display of FACET is presented in figure 20. In this figure, the yellow icons are used to represent the current position of aircraft flying in and around the United States, the red boundary is the outline of the lower 48 states, the white lines are the Air Route Traffic Control Center (ARTCC) boundaries, and the dark blue lines are the high-altitude sector boundaries.

To support the Hopper electric aerial vehicle study, FACET's waypoint adaptation database was updated to display all of the nodes in the initial Hopper network. An updated Bay Area coastal map database was added to the system to improve the data visualization aspects, and a capability was added to construct and visualize "flow corridors" in FACET between the various nodes in the proposed Bay Area network. New capabilities were also developed to allow FACET to read and process NCT air traffic data and, finally, new aircraft performance models were added to the system to allow 6-, 15- and 30-passenger Hopper vehicles to be simulated.

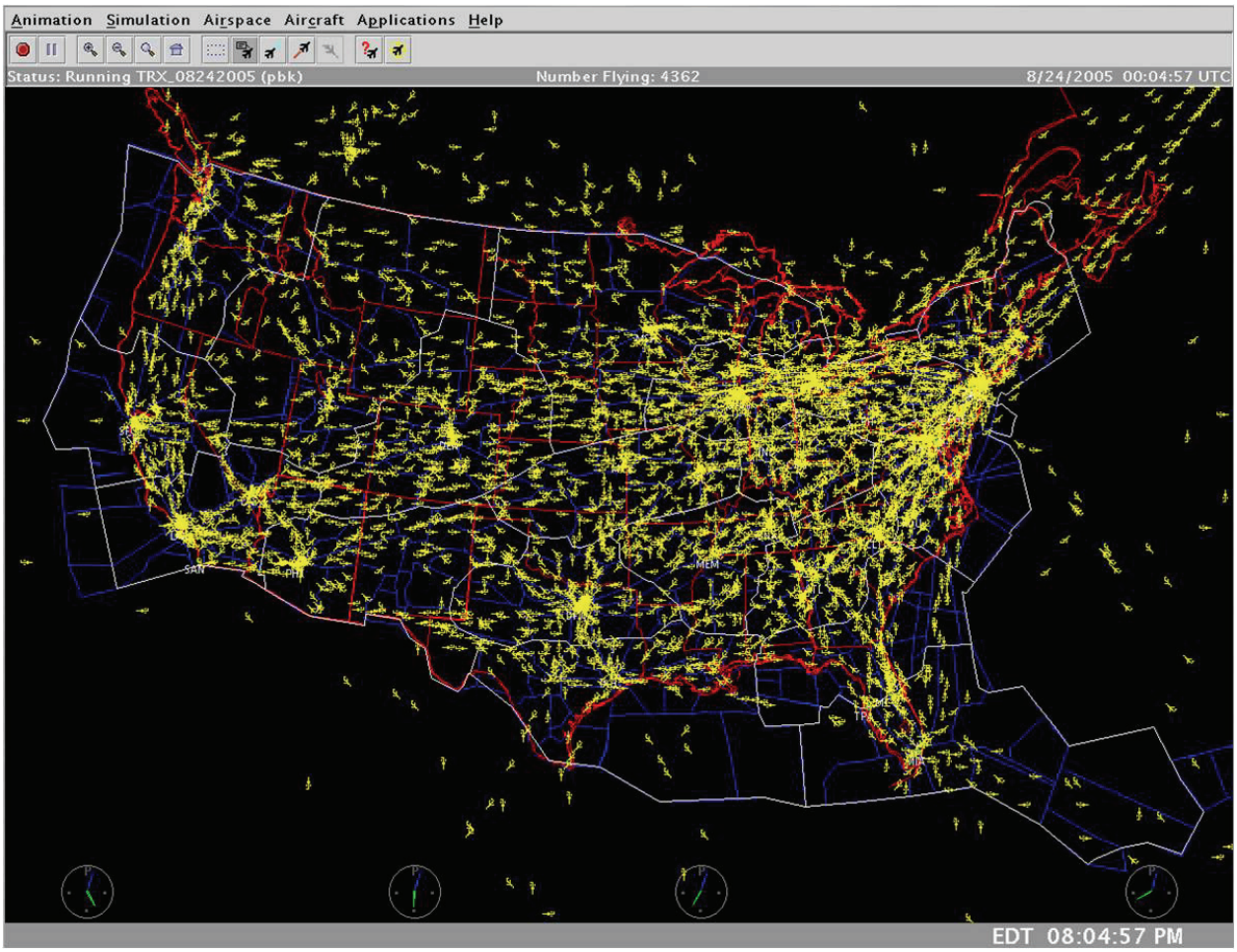

Figure 20. Future ATM Concepts Evaluation Tool (FACET) visualization of air traffic over the continental USA for a given instance of time.

B. Air Traffic Environment

Although the Hopper vehicles could conceivably operate within any metro-region in the country, for initial testing the vehicles were assumed to operate within the San Francisco Bay Area. The NCT controls low altitude and transitioning traffic within the San Francisco Bay Area. This facility handles 4,800–5,200 operations per day including 3 major airports, 73 public/municipal airports, and a vast number of private airports. The major San Francisco (SFO), San Jose (SJC) and Oakland (OAK) arrival and departure flows within the NCT are depicted in figure 21. As can be seen by comparing the flows in this figure with the Hopper network shown in figure 2, fairly significant interactions between the Hopper vehicles (ref. 21) and the air traffic flows are expected, and the extent of these interactions will be quantified later in this report.

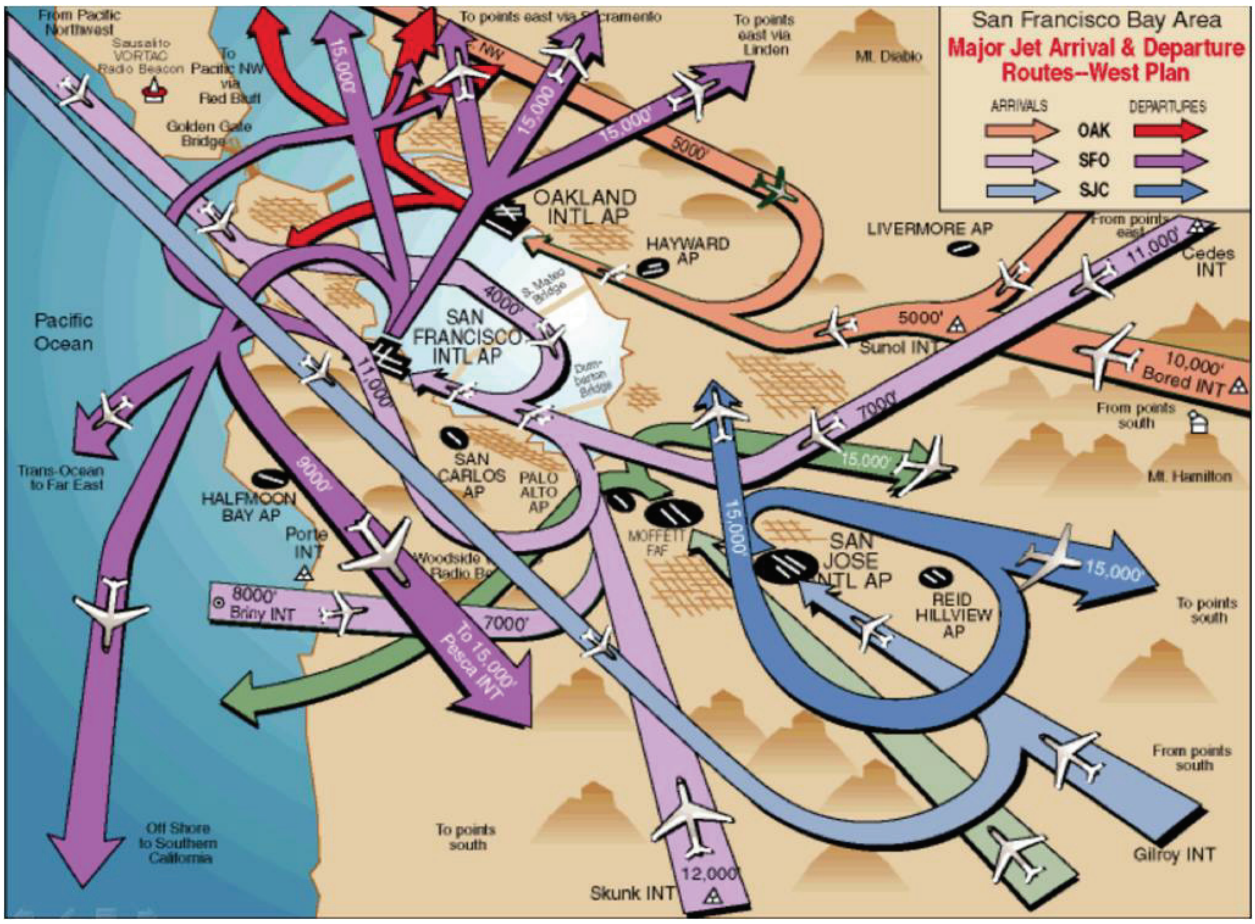

Figure 21. Major arrival and departure air traffic flows in the San Francisco Bay Area.

C. Aerial Transit System Air Traffic Scenario

To explore the combined interaction of the proposed Hopper vehicles and existing air traffic, FACET was employed in the analysis process schematically outlined in figure 22. FACET's trajectory prediction module was used to simulate the four-dimensional (4-D) trajectory of each Hopper vehicle from the vehicle's departure station to the destination station. For initial testing, the vehicles were assumed to fly a direct route from the departure point to the destination using great circle navigation. The simulated trajectories were subsequently recorded in an output file. The top three flowchart boxes in figure 22 depict the steps for creating and storing the simulated trajectories. The actual, historical positions of aircraft operating in the NCT are subsequently merged with the simulated Hopper trajectories as illustrated in figure 22, and this integrated data set is used in FACET's playback mode to explore the interaction between the Hopper vehicles and the existing background air traffic flows. For initial testing, the flights operating within the NCT on January 18, 2011, (a Tuesday) were used to represent typical background traffic flows, and all fast-time simulation experiments were run from 8:00 Universal Time Coordinated (UTC) to 24:00 UTC, which corresponds to 0:00 to 16:00 Pacific Standard Time (PST).

Figure 23 presents representative airspace results for a Hopper 5,000 minimum aircraft schedule integrated with the NCT traffic. As can be seen in figure 23, the Hopper traffic is a small but significant number compared to the total aircraft count for the NCT.

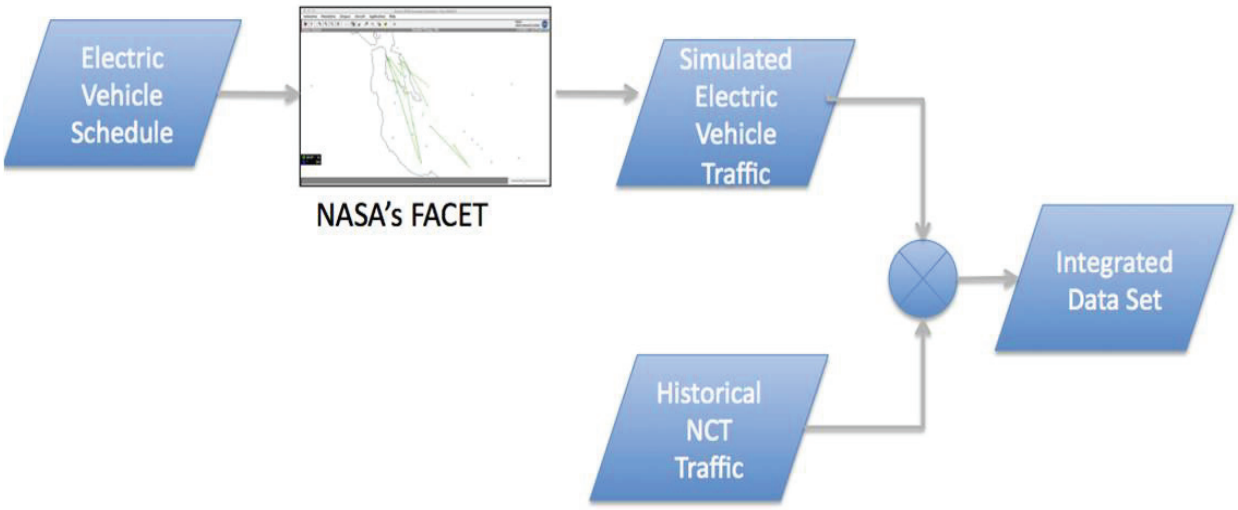

Figure 22. FACET process for creating and storing trajectory information.

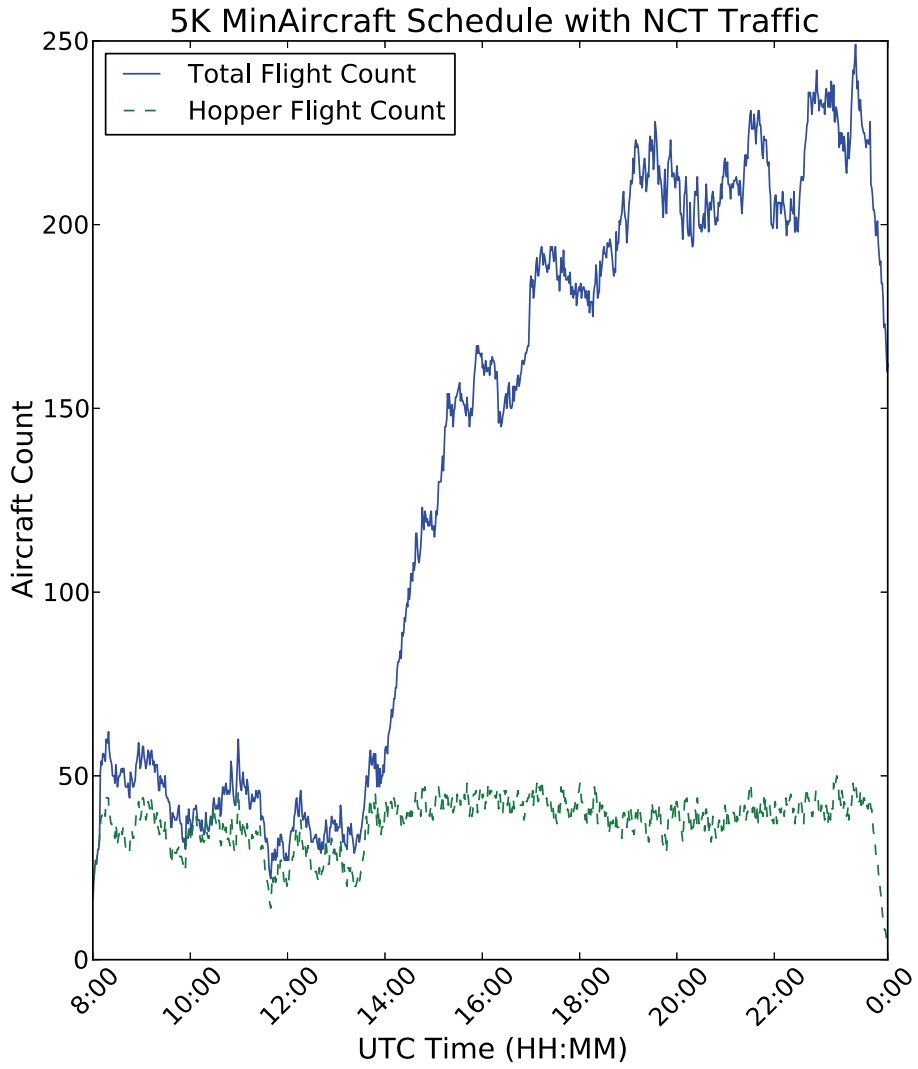

Figure 23. Aircraft counts.

D. Key FACET Analysis Metric: Loss of Separation

The primary means for quantifying the interaction between the simulated Hopper vehicles and the existing background air traffic flows was to measure the number of simulated loss-of-separation events. The rationale behind selecting this metric was that if the number of loss-of-separation events is low then (1) there is little safety concern associated with operating the Hopper vehicles in the presence of the background traffic flows; (2) there is little need for an air traffic controller to intervene and separate the vehicles, so controller workload is not increased; and (3) the need for special corridors in which to operate the Hopper vehicles will likely be unnecessary.

For the initial set of experiments, the TRACON Instrument Flight Rules (IFR) separation standards were used for detecting losses of separation. These separation rules are illustrated in figure 24, and these standards define a loss of separation as occurring when two aircraft come within 3 nm of one another in the horizontal plane and within 1,000 feet of one another in the vertical plane. The next section provides the results of the fast-time simulation experiments in terms of this metric.

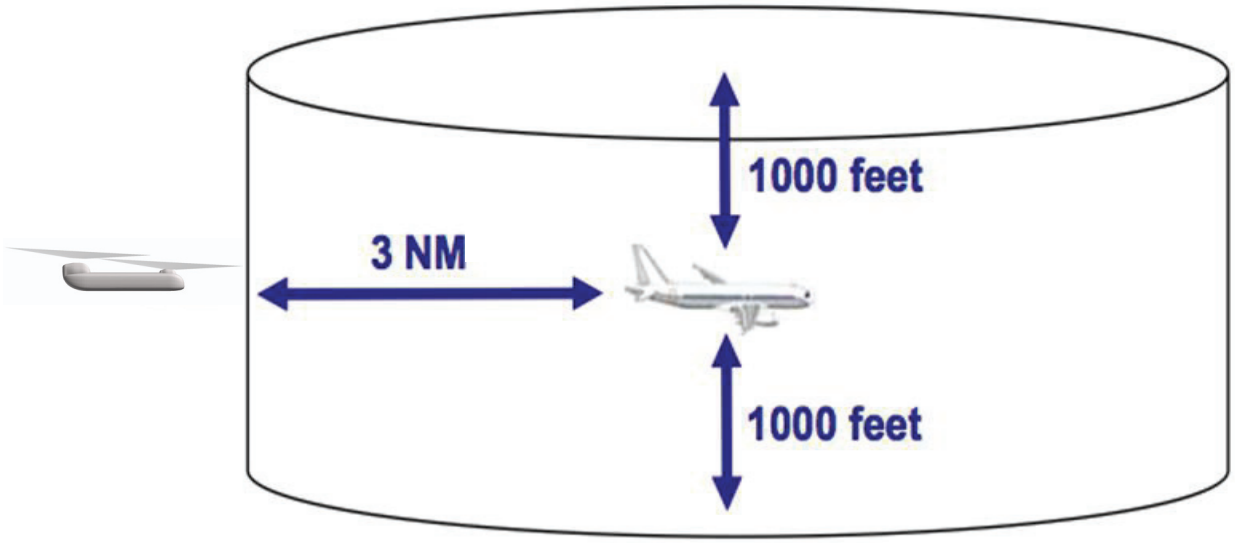

Figure 24. Loss-of-separation definition.

E. Airspace Simulation Results

In order to select a preferred altitude at which to operate the Hopper vehicles, at least from an air traffic perspective, the density of flights within the Bay Area at 1,000, 2,000, 3,000, and 5,000 feet was examined using the traffic density profiler in FACET. Using this capability, a 5-nm x 5-nm horizontal grid was overlaid across the Bay Area, and the cumulative number of flights observed within any one of the grid cells at the specified altitude level was calculated. The results of this analysis are shown in figure 25. The black cells are ones in which 10 or fewer aircraft were observed, the blue cells indicate that 10 to 20 aircraft passed through the cell, the green cells indicate that 20 to 30 aircraft passed through the cell, and yellow cells indicate that 30 to 40 aircraft passed through the cell. Figure 25a shows a yellow cell roughly over Palo Alto, CA, at 1,000 feet, which indicates the relatively high level of activity around the Palo Alto Airport due to general aviation traffic. These same general aviation flights are also largely responsible

for the two green cells appearing in figure 25b at 2,000 feet. The traffic densities at 3,000 feet, shown in figure 25c, are relatively low and uniform compared to lower altitudes, while the arrival and departure flows to/from SFO and SJC start to become visible in figure 25d at 5,000 feet, as indicated by the two green cells. Because of the relatively uniform, low densities that were observed at 3,000 feet on this particular day, this is likely the best altitude at which to operate the Hopper vehicles if they are assumed to fly great circle routes at a constant altitude from their starting node to their destination nodes. In follow-on work, more sophisticated horizontal and vertical trajectories will be explored that minimize the interaction between the Hopper vehicles and the background air traffic flows. When developing these alternative trajectories, it will be essential to ensure that the trajectories are suitable for a Hopper vehicle that is designed for mass transit use, and that the alternative trajectories do not impact the Hopper network schedule that was previously discussed.

A summary of the loss-of-separation events for nine different 16-hour fast-time simulation experiments is presented in figure 26. Here the flight level at which the Hopper vehicle is cruising at, and the number of passengers being serviced by the network, is being varied. As can be seen from figure 26, operating the Hopper vehicles at FL30, or 3,000 feet, minimizes the total number of loss-of-separation events, and, in general, the number of loss-of-separation events grows approximately linearly with the number of passengers serviced by the network. As previously mentioned, follow-on research that is designed to optimize the horizontal and vertical trajectories of the Hopper vehicles, while taking into account the background traffic flows, is likely to significantly reduce the number of loss-of-separation events.

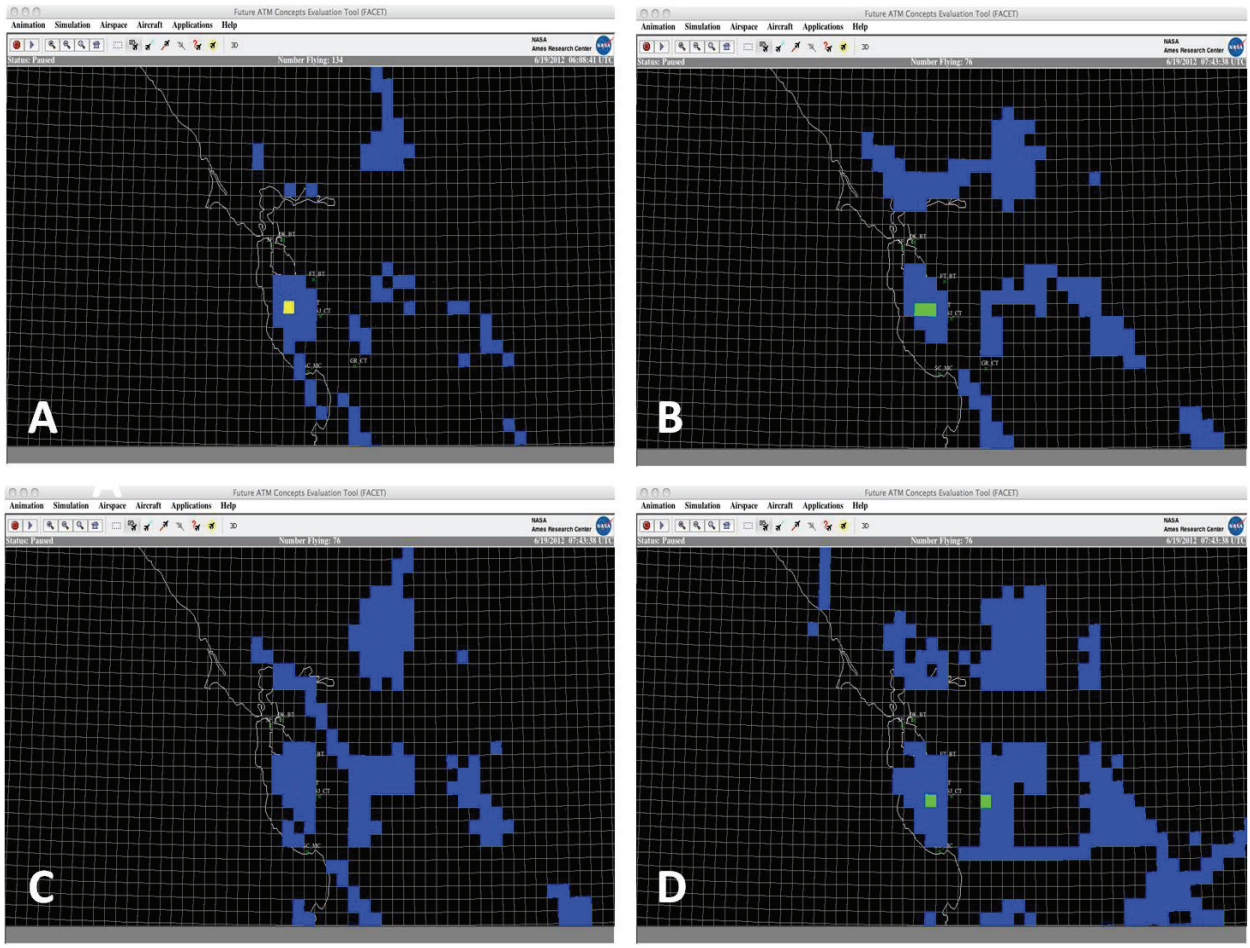

Figure 25. Traffic density plots at (a) 1,000 ft, (b) 2,000 ft, (c) 3,000 ft, and (d) 5,000 ft.

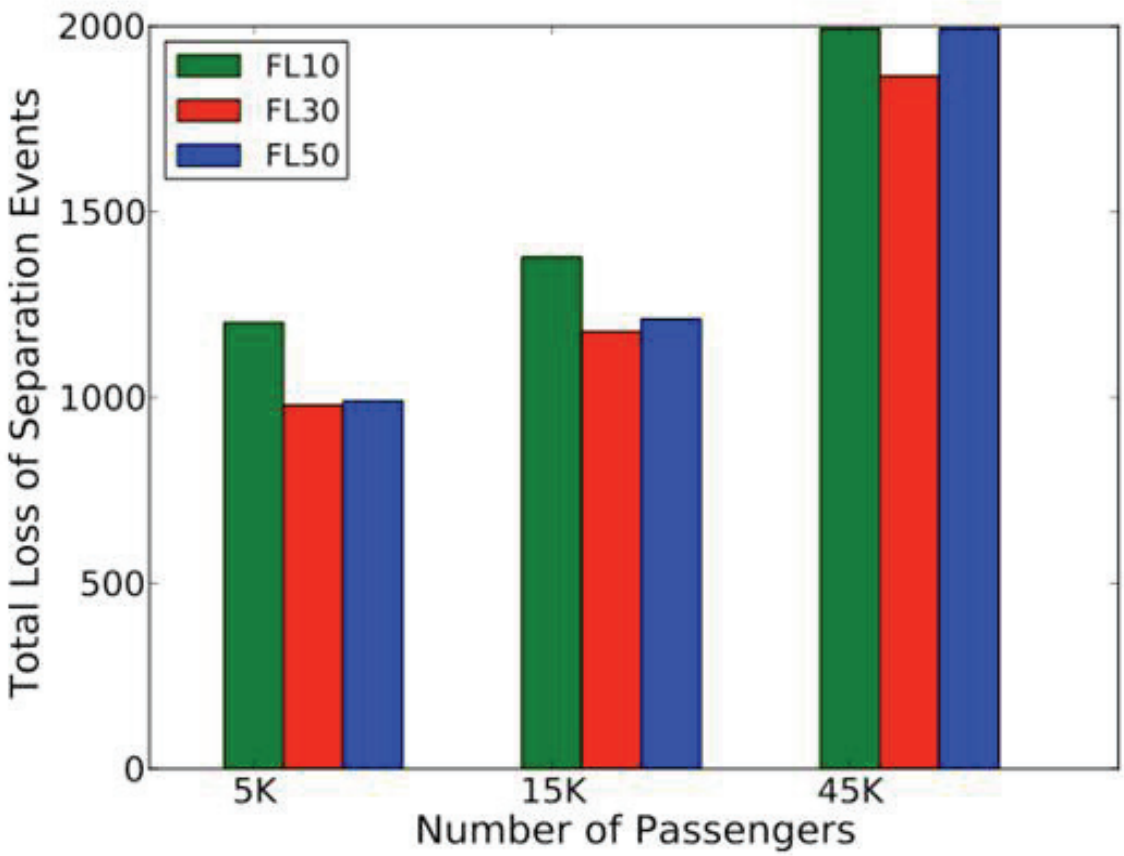

Figure 26. Loss-of-separation events as a function of the number of passengers and the Hopper vehicle cruise altitude.

VI. Summary

NASA and Stanford University jointly performed an aerial mass transit feasibility study. The conceptual design of an electric VTOL vehicle suitable for the aerial mass transit system was explored. The conceptual design was completed in the context of the study's larger multidisciplinary scope, which examined the overall system feasibility in the context of air vehicle design, passenger throughput, and impact on the surrounding airspace. As a part of this study, the value of a multidisciplinary system-level approach to design is seen in the various potential trade-offs that have been presented in the results. Network topology, scheduling, and air traffic integration are not typically considered at the conceptual design level, but have been shown to provide constraints and important measures of performance that impact the design mission profile and aircraft sizing. Selection of design parameters such air vehicle range, cruise altitude, and passenger capacity need to be considered in the context of system-wide metrics such as the number of airspace loss-of-separation events and passenger-demand behavior, in addition to vehicle performance and cost metrics.

Models, tools, and processes have been created to simulate a baseline airborne commuter transportation system. The baseline network and fleet were specified so as to identify issues, trends, and focus; it is not an optimal system. Rotorcraft have been designed specific to the extreme short haul routes of the notional metro-regional aerial transit system. Conventional propulsion designs "close" at 6-, 15-, and 30-passenger-size vehicles with current technologies. Electric propulsion designs at 6- and 15-passenger counts are projected to close using +15 year

technology development. Electric propulsion designs at the 30-passenger size are projected to close using +30 year technology development based on this study's results; it is postulated that 30-passenger VTOL vehicles are the upper bound of size for electric propulsion. Without optimizing the network topology and while servicing 24-7 ridership, the following insights have been gained from work to date: larger ridership drives toward a uniform fleet of 30-passenger vehicles; aerial transit system optimization will be driven by number of aircraft at-station (i.e., footprint) as this will have significant implications as to vertiport station infrastructure costs (a maximum of approximately 50 aircraft at-station at the San Francisco vertiport was projected under certain simulation scenarios); there is large airspace conflict at 5,000 feet therefore lower altitude operations, or alternate approaches, will be required to lower airspace loss-of-separation conflicts, but at a potential cost of greater community noise; through the use of the BaySim, FACET and network topology tools have simulated up to 45,000 daily riders (equal to CalTrain ridership but transporting them over 2.5 times the average distance).

To realize such a novel metro-regional aerial transportation system, a number of key technology challenges need to be met. Battery technology, though seeing considerable advances over the past several years, is currently focused on the consumer electronics and automotive industries. Aviation applications, particularly as related to propulsion, will entail unique and technologically challenging design requirements. For example, higher specific energy battery technology is a key enabler for the air vehicle designs. In addition to the issues investigated in this study, there are several other important considerations in the potential realization of a Hopper-like network. Historically, conventional rotorcraft have not been economically competitive compared to fixed-wing aircraft. Further, rotorcraft noise is a significant impediment to passenger and community acceptance. Technology advances in automation, onboard vehicle health monitoring, drive train components and vehicle structures, and rotor noise reduction will all be required to enable the type of metro-regional aerial transit system studied in this report.

To conclude, it seems possible that extreme short haul rotorcraft could be an element of metro-regional commuter travel. Conventional propulsion rotorcraft could be employed today. Electric propulsion will require technology development and still likely have a relatively limited passenger carrying capacity. There seems to be potentially sufficient ridership capacity in the aerial transit network design studied to transport thousands of daily riders.

VII. Future Work/Continued Study

Given the successful development of an analytical framework in this reported effort (Phase I), a continued study effort is being performed (Phase II; ref. 36). The scope of this continued study is to take the analytical tools and analyses developed in this reported effort and to seek to determine the most feasible approach to one day develop a realizable network of station-to-station VTOL/aerial vehicles—ideally employing electric propulsion—serving the transportation needs of urban metropolises.

Consistent with the above noted scope, a set of objectives is defined. Each objective is linked to addressing four fundamental questions regarding the feasibility of the overall aerial transportation concept. First, can one or more business cases be developed that establishes the feasibility of the proposed concept (in the near-, mid-, and far-term time frames)? Second, beyond the economics of the proposed concept, are there other positive societal attributes that may enable its adoption? Third, what are the critical, unique, and NASA-only enabling technologies for air transportation networks, including the development of VTOL environmentally friendly propulsion systems? And, finally, fourth, can this proposed work be ultimately integrated or, rather, transitioned—and how to best do so—into the main ARMD

projects so as to maximize the probability that one day such an urban air transportation system might be developed?

To meet these objectives, the following technical approach and associated tasks are being actively pursued:

1. Refinement and Extension of Network Design/Tools

This task will consist of refining and extending the network design/tools. Airspace operations and the network design are being more fully considered as compared to what was possible in this reported effort. The network topology and its variations will be examined from an on- and off-nominal set of operational conditions. The network analysis tool of choice will continue to be the BaySim tool. The network topology of this reported effort was based on point-to-point operation. The continued study effort will examine alternative network topologies including hub and spoke configurations. Hub and spoke configurations might be advantageous for (at least) two reasons: 1) overall throughput and 2) number of aircraft on station. If the number of aircraft (aircraft footprint) at a given station becomes too large, it will significantly increase infrastructure—including real estate—cost. As a part of this expanded network analysis, the concept of dynamic routing will be examined, based on either a station going off-line or a surge of traffic at a given location. Finally, the safety implications of the aircraft fleet mix and network configuration will be considered. Another key consideration, in terms of airspace analysis, is the question of optimizing (qualitatively, at least) the altitude and flightpaths of the fleet of aerial vehicles to minimize interference/conflict with conventional aircraft. The tool of choice will continue to be the FACET software. This reported effort fixed the fleet cruise altitude at 5,000 feet; consequently, the airspace simulations using the FACET tool showed a high potential at that cruise altitude for interfering flights for the larger projected fleets. This issue will be studied in more detail in the follow-on effort.

2. Refinement and extension of vehicle and fleet designs/tools

Refine the network/vehicle fleet designs on the basis of the results from the below noted alternative business case analysis. In particular, what would a near- to mid-term network/fleet look like versus a mid- to far-term network/fleet? A Stanford-developed conceptual design tool, validated against this effort's NDARC results, will be used for the follow-on vehicle/fleet analysis/sizing. In particular, steps will be taken to ensure that the baseline (combustion-based propulsion) fleet is made consistent with a near- to mid-term implementation of the station-to-station (extreme short haul) urban aerial vehicle network. Electric-propulsion vehicles can have a longer-term focus, if need be, for possible implementation. This would entail both improvements to tools, as well as conceptual designs employing a design-by-simulation methodology. This task would also look at alternate propulsion concepts such as hybrid (combined electric and combustion-based) systems, fuel-cell-based systems, etc. The risks and benefits and ease-of-introduction of these alternate propulsions systems would be considered in this task. As a part of this analysis, the system energy intensity (BTU/PX-mile) of the various vehicle fleet and network options will be assessed.

3. Alternate Business Models

Conduct an assessment of multiple alternate business models for proposed extreme short haul concept. A local AHS (American Helicopter Society) International chapter seminar was recently given in which the Chief Executive Officer (CEO) of a Vancouver, BC, helicopter air taxi (one of the few existent non-EMS/petroleum/tourism-focused helicopter transport

service companies) discussed the challenges and opportunities of providing economically viable urban helicopter services. It would be interesting to see if some of the analysis tools developed and study results generated could help the helicopter industry develop viable business models to enable such “extreme short haul” markets for trips less than 100 miles. The electric vehicle and the extreme short haul concepts need to be explored somewhat independently from each other—e.g., electric vehicles might not be economically viable in the near- to mid-term time frames but fossil-fuel-propelled vehicles might be. Ultimately, though, electric and/or green propulsion concepts should be the long-term goal for implementation.

4. Aerial Vehicle Station Design and Operations

This task consists of the conceptualization and assessment of infrastructure—and operational—requirements for proposed urban aerial transport system(s). Key among the issues considered in this task is the aerial vehicle station design and operations: In order to drive down the mass of the vehicles, it is important to carry as little power (fuel) as possible while still meeting mission requirements. Among the station design issues to be considered (for the electric-propulsion version of the vehicle fleet) is the question of periodically recharging the vehicles at the (ground) stations; the initial ideas considered in this reported effort were either using quick-charge equipment or some sort of automated battery swap.

5. Technology Roadmap

Develop a technology roadmap for the unique technologies and capabilities required for the success of the concept. Roadmap would include not only electric propulsion technologies but, perhaps, automation and autonomous system technology. (Personnel costs are likely to be a big driver of operational costs for such a network. If the network is dominated by proscribed and time-regulated station-to-station flights, then vehicle autonomy might be a make-or-break vehicle capability.) Ultimately such a roadmap should complement and, ideally be integrated into, NASA’s mainstream aeronautics technology portfolios and demonstrations opportunities.

6. Concept/CONOPS Implementation Roadmap

This task consists of two parts. First, a notional implementation plan will be developed. In this notional plan, there will likely be an early network of semi-on-demand and semi-scheduled fleet of conventional propulsion (non-electric) rotary wing aircraft for high-value point-to-point flights. This network would then evolve to one having higher capacity traffic with more frequently scheduled flights. The later stages of this network would first adopt small, and then increasingly larger, vehicles with electric propulsion and, in turn, network topologies more in kind to mass public transit models. Second, the task will explore integration of extreme short haul concept business models and CONOPS with the notional “Civil Tiltrotor in NextGen” CONOPS (refs. 37,38). This notional integration effort would seek to overall improve the door-to-door time and economic competitiveness of both concepts/CONOPS.

This overall effort directly addresses NASA’s strategic goals to advance aeronautics research for societal benefit. Transportation is a first-order driver to the economy; a lower cost and adaptive metro transportation system would have a first-order effect on regional economies and direct economic benefit to the nation. The proposed work has direct relevance to a number of ARMD programs/projects, including a possible tie-in/transition to the NASA rotary wing research efforts. Additionally, the reported conceptual design efforts could potentially factor into vehicle and CONOPS demonstrations.

References

[1]Seeley, B.A.: Faster and Greener – Pocket Airports. Nov. 8, 2010; CAFE Foundation website, http://www.cafefoundation.org/public/2010_08_16/P8.Essay.Final_sm.pdf; accessed Sept. 10, 2013.

[2]Anom.: Systems Analysis of Short Haul Transportation. Massachusetts Institute for Technology Flight Transportation Laboratory, TR 65-1, 1965.

[3]Wood, C. C.: Vertical Takeoff Aircraft for Metropolitan and Regional Service. *AIAA 4th Annual Meeting and Technical Display*, AIAA 67-940, Anaheim, CA, 1967.

[4]Anom.: Transportation by Helicopter: 1955–1975. Port Authority of New York, 1952.

[5]Johnson, W.: NDARC: NASA Design and Analysis of Rotorcraft. NASA/TP-2009-215402, 2009.

[6]Moodie, A. M. and Yeo, H.: Design of a Cruise-Efficient Compound Helicopter. J. American Helicopter Society, vol. 57, no. 3, July 2012.

[7]Russell, C. and Johnson, W.: Application of Climate Impact Metrics to Civil Tiltrotor Design. 51st AIAA Aerospace Sciences Mtg., Grapevine, TX, Jan. 7–10, 2013.

[8]PASS: Program for Aircraft Synthesis Studies, http://adg.stanford.edu/aa241/pass/pass1.html; accessed Nov. 26, 2013.

[9]Caltrain Local Commuter Rail, http://www.caltrain.com, accessed Jan. 30, 2013.

[10]Bay Area Rapid Transit (BART) System, http://www.bart.gov, accessed Jan. 30, 2013.

[11]Nance, R.E.: A History of Discrete Event Simulation Programming Languages. Bergin, T. and Gibson, R. (Eds.), *History of Programming Languages II*, ACM Press, New York, 1996.

[12]Bazargan, M.: *Airline Operations and Scheduling*. Ashgate Publishing Limited, Surry, England, 2010.

[13]Hane, C.; Barnhart, C.; Johnson, E.; Marsten, R.; Nemhauser, G.; and Sigismondi, G.: The Fleet Assignment Problem: Solving a Large-Scale Integer Program. *Mathmatical Programming*, vol. 70, no. 1–3, 1995, pp. 211–232.

[14]Bilimoria, K.; Sridhar, B.; Chatterji, G.; Sheth, K.; and Grabbe, S.: Future ATM Concepts Evaluation Tool. Air Traffic Control Quarterly, vol. 9, no. 1, Mar. 2001.

[15]Johnson, W.; Yamauchi, G.K.; and Watts, M.E.: NASA Heavy Lift Rotorcraft Systems Investigation. NASA/TP-2005-213467, 2005.

[16]Chretien, P.: The Quest for the World's First Electric Manned Helicopter Flight: From Concept to Prototype in 180 Days. *Vertiflite*, vol. 58, no. 2, 2012, pp. 38–42.

[17]Dudley, M.: Promising Electric Aircraft Drive Systems. *EAA Electric Aircraft World Symposium*, ARC-E-DAA-TN2019, Oshkosh, WI, 2010.

[18]Jost, M.: UAV Flight Time Increased By 80% Using New High Energy Battery System. *Press Release*, SION Power, Tuscon, AZ, June 21, 2011.

[19]Gunston, B.: General Electric CT7. *Jane's Aero-Engines*, 19th ed., Jane's Information Group Limited, UK, 2006, pp. 574–578.

[20]Dudley, M. and Misra, A.: Electric Airplane Power-system Performance Requirements. The 2009 CAFE Foundation Electric Aircraft Symposium, Hiller Aviation Museum, San Carlos, CA, April 24, 2009; http://cafefoundation.org/v2/pdf_eas/2009/MichaelDudley_2009.pdf; accessed Sept. 8, 2014.

[21]Synder, C., et al.: Propulsion Investigation for Zero and Near-Zero Emissions Aircraft. NASA TM-2009-215487, 2009.

[22]McClintock, J. and Holbrook, J.: Alternative Fuels: Taking A Second Look at Ammonia. National Defense, Aug. 2008; http://www.nationaldefensemagazine.org/archive/2008/August/Pages/AlternativeFuelsTakingASecondLookatAmmonia.aspx; accessed Sept. 8, 2014.

[23]Datta, A. and Johnson, W.: Requirements for a Hydrogen Powered All-Electric Manned Helicopter. *12th AIAA Aviation Technology, Integration, and Operations (ATIO) Conference*, Indianapolis, IN, Sept. 17–19, 2012.

[24]Automated Automotive-class Battery Swap Technology Demonstration/Option: http://www.teslamotors.com/batteryswap; accessed Dec. 27, 2013.

[25]Leishman, J.G.: *Principles of Helicopter Aerodynamics*. Cambridge University Press, 2006, p. 66.

[26]Glaze, K.: Vertical Flight Passenger Services: Past, Present and Future. *Presented to the San Francisco Bay Area Chapter of the AHS*, Moffett Field, CA, Mar. 7, 2012.

[27]FAA: FAR Part 29, One-Engine-Inoperative Category A Rotorcraft Operations; http://www.faa.gov/regulations_policies/rulemaking/committees/documents/media/R2729T1-121192.pdf; accessed Sept. 8, 2014.

[28]Johnson, W.: *Rotorcraft Aeromechanics*. Cambridge University Press, 2013, p. 12.

[29]Estimates of 2008 Number of “Tech Industry” Workers: http://www.marketwatch.com/story/silicon-valley-and-ny-still-ride-high-in-cybercities-rankings; accessed Sept. 24, 2014.

[30]CalTrain Ridership Passenger Levels: http://www.caltrain.com/about/statsandreports/Ridership.html; accessed Aug. 5, 2014.

[31]Cetin, N.; Burri, A.; and Nagel, K.: A Large-Scale Agent-Based Traffic Microsimulation Based on Queue Model (2003). Proceedings of Swiss Transport Research Conference (STRC), Monte Verita, CH, 2003.

[32]Savage, J.E.: *Models of Computation: Exploring the Power of Computing*, Addison-Wesley Longman Publishing Co., Inc. Boston, MA, 1997.

[33]Hane, C.A.; Barnhart, C.; Johnson, E.L.; Marsten, R.E.; Nemhauser, G.L.; and Sigismondi, G.: The Fleet Assignment Problem: Solving a Large-Scale Integer Program. Mathematical Programming, vol. 70, no. 1–3, Oct. 20, 1995, pp. 211–232.

[34]Subramanian, R.; Scheff, R.P.; Quillinan. J.D.; Wiper, D.S.; and Marsten, R.E.: Coldstart: Fleet Assignment at Delta Air Lines. Interfaces, vol. 24, no. 1, Jan.–Feb. 1994, pp. 104–120.

[35]Gurobi Optimization Software: http://www.gurobi.com/resources/free-linear-programming-solvers; accessed Sept. 3, 2014.

[36]Alonso, J.J.; Arneson, H.M.; Kontinos, D.A.; Melton, J.E.; Sinsay, J.D.; Tracey, B.; Vegh, M.; Walker, C.T.; and Young, L.A.: System-of-Systems Considerations in the Notional Development of a Metropolitan Aerial Transportation System: Implications as to the Identification of Enabling Technologies and Reference Designs for Extreme Short Haul VTOL Vehicles with Electric Propulsion. NASA TM 2014-xxxxxx (soon to be published).

[37]Chung, W.W., et al.: Modeling High-Speed Civil Tiltrotor Transports in the Next Generation Airspace. NASA/CR-2011-215960, Oct. 2011.

[38]Chung, W.W., et al.: An Assessment of Civil Tiltrotor Concept of Operations in the Next Generation Air Transportation System. NASA/CR-2012-215999, Jan. 2012.

Appendix—BaySim Hopper Network Modeling

A. Implementation With Finite State Machines

The basic elements of a simple DES for passengers (PX) in a transportation network are illustrated in the pseudocode (fig. A1) below:

START

INITIALIZE PX population

INITIALIZE air terminal network

UPDATE clock

LOOP over flights

Set flight behavior using FSM to update and transition each flight through three states based on clock, PX queues, and current state

END LOOP

LOOP over PX population

Set PX behavior using FSM to update and transition each PX through fourteen states based on clock, position, and current state

END LOOP

UPDATE PX queues for those awaiting flights

COMPUTE population statistics

DRAW graphics

APPEND PX and flight logfiles

REPEAT clock

STOP

Figure A1. Pseudocode for BaySim Discrete Event Simulation.

B. Agent/Passenger Characteristics

The passenger population is composed of three primary groups, with each group assigned to a day, evening (swing), or night (graveyard) work shift. The day shift is worked by 70 percent of the passenger population, the evening shift by 20 percent, and the night shift by 8 percent. The remaining 2 percent of passengers are assigned a random work shift. Within each shift, individual passengers are then further assigned a daily wake-up time, a ground speed at which that passenger travels to his/her departure air terminal, a ground speed for travel from the arrival air terminal to the workplace, a time required to remain at the workplace, and similar values for their return trip back home. Gaussian randomness is applied to each of these inputs.

A finite state machine (FSM) was used within the DES in order to simulate the various behaviors of passengers. During the 24-hour day, each passenger in the population transitions through nine states of behavior. The transition between states occurs as a function of current clock time, current state, and current position within the transportation network. These passenger states are as follows:

AtHome,
AtWork,
SurfaceTravelFromHome,
SurfaceTravelToWork,
SurfaceTravelFromWork,
SurfaceTravelToHome,
QueuedAtHomeStation,
QueuedAtWorkStation,
QueueDelayReturningHomeFromHomeStation,
QueueDelayReturningHomeFromWorkStation,
HomeStationToWorkStation, and
WorkStationToHomeStation.

The passenger states and their transition criteria are illustrated in table A1. The transition criteria are checked every clock step.

Table A1.Passenger States

Passenger State: px_State[i]	Next State	Transition Condition	Notes
AtHome	SurfaceTravelFromHome	SimClock >= p_DayStart[i] + 0.5 * Math.random()	Leave home for work after a certain time each day
SurfaceTravelFromHome	QueuedAtHomeStation	p_distToGo[i] <= 0	Travel from home to the departure node
QueuedAtHomeStation	HomeStationToWorkStation	p_foundARide[i] == true	Queued at the departure node, queue meets load factor requirements for departure flight, load/departure time delay has passed
QueuedAtHomeStation	QueueDelayReturningHomeFromHomeStation	SimClock - p_QueueStartTime[i] > p_GoBackHome[i]	Exceeded time limit for finding a flight after queueing at node, decide to return home
QueueDelayReturningHomeFromHomeStation	AtHome	p_distToGo[i] <= 0	Destination is home, surface transport
HomeStationToWorkStation	SurfaceTravelToWork	p_distToGo[i] <= 0	Fly between nodes (home to work), Arrival delay has passed
SurfaceTravelToWork	AtWork	p_distToGo[i] <= 0	Travel to workplace from arrival node
AtWork	SurfaceTravelFromWork	SimClock >= p_WorkUntil[i]	Stay at workplace for a predefined time
SurfaceTravelFromWork	QueuedAtWorkStation	p_distToGo[i] <= 0	Travel from workplace back to arrival node
QueuedAtWorkStation	WorkStationToHomeStation	p_foundARide[i] == true	Queued at the arrival node, queue meets load factor requirements for return flight, Departure time delay has passed
QueuedAtWorkStation	QueueDelayReturningHomeFromWorkStation	SimClock - p_QueueStartTime[i] > p_GoBackHome[i]	Exceeded time limit for finding a flight after queueing at node, decide to return home via ground transport
QueueDelayReturningHomeFromWorkStation	AtHome	p_distToGo[i] <= 0	Surface travel from arrival node back to home
WorkStationToHomeStation	SurfaceTravelToHome	p_distToGo[i] <= 0	Fly between nodes (work to home), unload /arrival delay has passed
SurfaceTravelToHome	AtHome	p_distToGo[i] <= 0	Travel from the departure node back to home

C. Simulation Geographic Constraints

Home and workplace locations for each passenger were assigned in a semi-random manner around each air terminal and workplace while maintaining a rough fidelity to the Bay Area population centers. Future BaySim simulation work will include improvements to these home and workplace distributions using official census data. Figure A2 shows an initial distribution of passengers (green markers), air terminals (yellow triangles), and workplace locations (black markers) for a ridership population of 40,000 commuters. The geographic locations of the air terminals were chosen to coincide with major existing Bay Area transportation hubs (usually CalTrain or BART stations). Passengers were assigned to their departure air terminals based on proximity. Workplaces for each passenger were assigned randomly, but the arrival air terminal was based on workplace proximity.

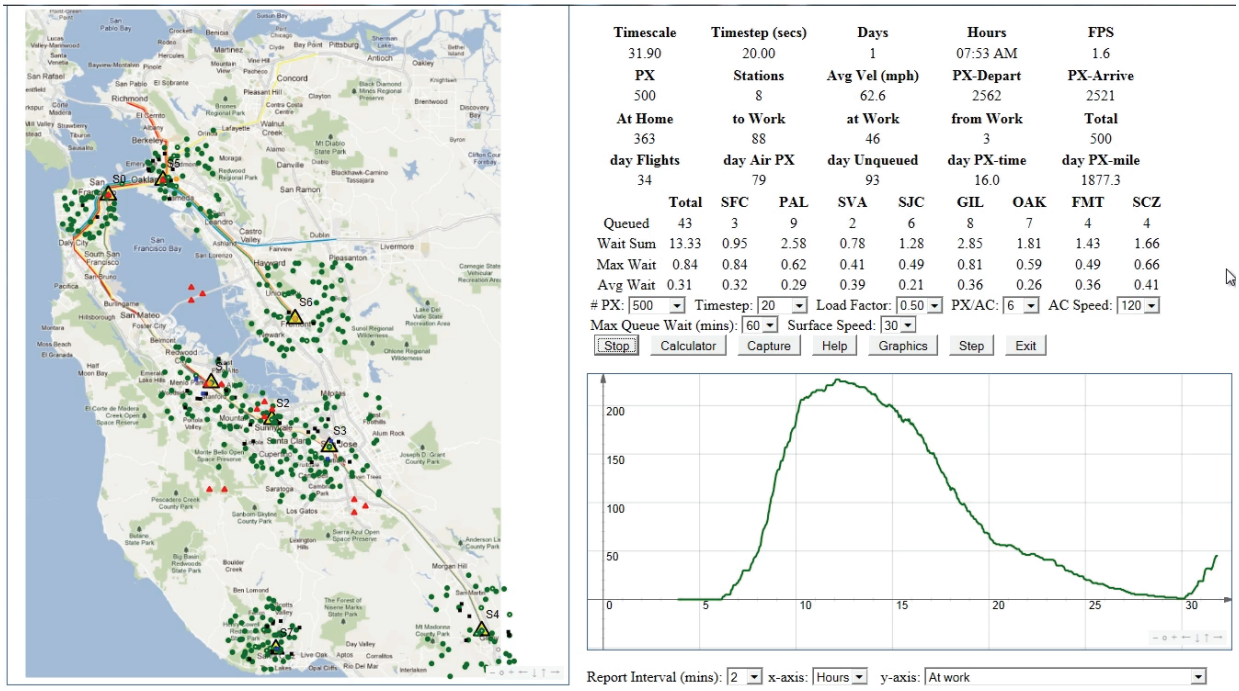

Figure A2. Another BaySim screen capture (later in the morning commute as compared to figure 7 in the main body of the report).

D. Simulation Aircraft Queuing Strategy

After using surface transportation to travel to a network node, passengers are queued up for flights according to their origin-destination (O-D) pairing. The logic behind the queuing strategy is presented in the pseudocode (fig. A3) below.

LOOP *over queued O-D lists of passengers* // "PX" = passengers {

/* Step 1: Completely fill aircraft using all available seats whenever possible and assign state as ready for takeoff because each seat is filled */

WHILE (#_of_PX_in_O-D_queue > max_#_of_PX_per_A/C) {

create a new flight_event *with state* = "ReadyForTakeoff";

assign PX to this flight_event;

compute estimated first departure time for the new flight_event based on the greater of (the time available due to the sum of PX loading and pushback delays) **OR** (next available departure time for this origin station);

remove PX from O-D queue;

compute next available departure time slot for this origin station;

}

/* Step 2: Assign remaining passengers to an aircraft if minimum load factor is met or if there is at least one passenger in the queue and the average wait time for that queue is greater than 30 minutes. Assign the state for the new flight to indicate that seats are available for any passengers who arrive before the departure time */

IF [(#_of_PX_in_O-D_queue > required_LoadFactor * max_#_of_PX_per_A/C) **OR** (#_of_PX_in_O-D_queue > 1 AND avgQueueWait > 0.5 hrs)] {

create a new flight_event with state = "SeatsAvailable";

assign PX to this flight_event;

compute departure time based on the greater of (*the time due to loading and pushback for current passengers*) **OR** (*next available departure time for this origin station*)

remove PX for O-D queue;

compute next available departure time for this origin station;

}

}

NEXT *O-D queue list*

Figure A3. Pseudocode for passenger queuing.

E. Simulated Hopper Aircraft Flight States

The rules determining the transitions between the three flight states are presented in table A2. Once an “EnRoute” flight reaches its destination, the arrival time is saved in an event log, and the flight event is removed:

Table A2. Simulation Flight State Rules

Flight State: flight_State[i]	***Next State***	**Transition Condition**	**Notes**
SeatsAvailable	ReadyForTakeoff	SimClock > DepartureTime, #PX == TotalSeats	Load passengers from queue up until departure time, being careful to ensure adequate boarding time
ReadyForTakeoff	EnRoute	SimClock > DepartureTime	PX loaded, awaiting scheduled departure time
EnRoute		p_foundARide[i] == true	Queued at the departure node, queue meets load factor requirements for departure flight, load/departure time delay has passed

F. Simulation Flight Departure Strategy

Using the states assigned to each flight, the logic behind flight departures is presented in the following pseudocode (fig. A4).

```
LOOP over flights {
        STATE "ReadyForTakeoff"
                …
                STATE "SeatsAvailable"
                IF ( clock + dt >= flightDepartureTime[i] ) {    // departure at next timestep
                      flightState[i] = "ReadyForTakeoff";
                } ELSE
                {
                        IF new passengers have come into the queue for this flight O-D pair {
                      IF there is time available for boarding {
                         compute number of passengers that can be loaded before pushback;
                              add these passengers to the flight and remove them from the queue;
                      }
                      IF the flight is now full {
                          flightState[i] = "ReadyForTakeoff";
                      }
                  }
               }
                STATE"EnRoute"
                …
}
NEXT flight
```

Figure A4. Pseudocode for flight departures.

G. Simulated Vehicles

Figure A5 is an illustration of the relative sizes and types of vehicles comprising the fleet studied. Both the 6- and 15-passenger vehicles are single main rotor and tail rotor helicopters. All vehicles incorporated in the BaySim simulations employed battery-powered electric-propulsion.

Figure A6 presents a set of power-required-versus-airspeed curves for the three passenger-size classes of Hopper vehicles studied. The power curves in figure A6 were generated by the NDARC vehicle sizing, design, and analysis software tool.

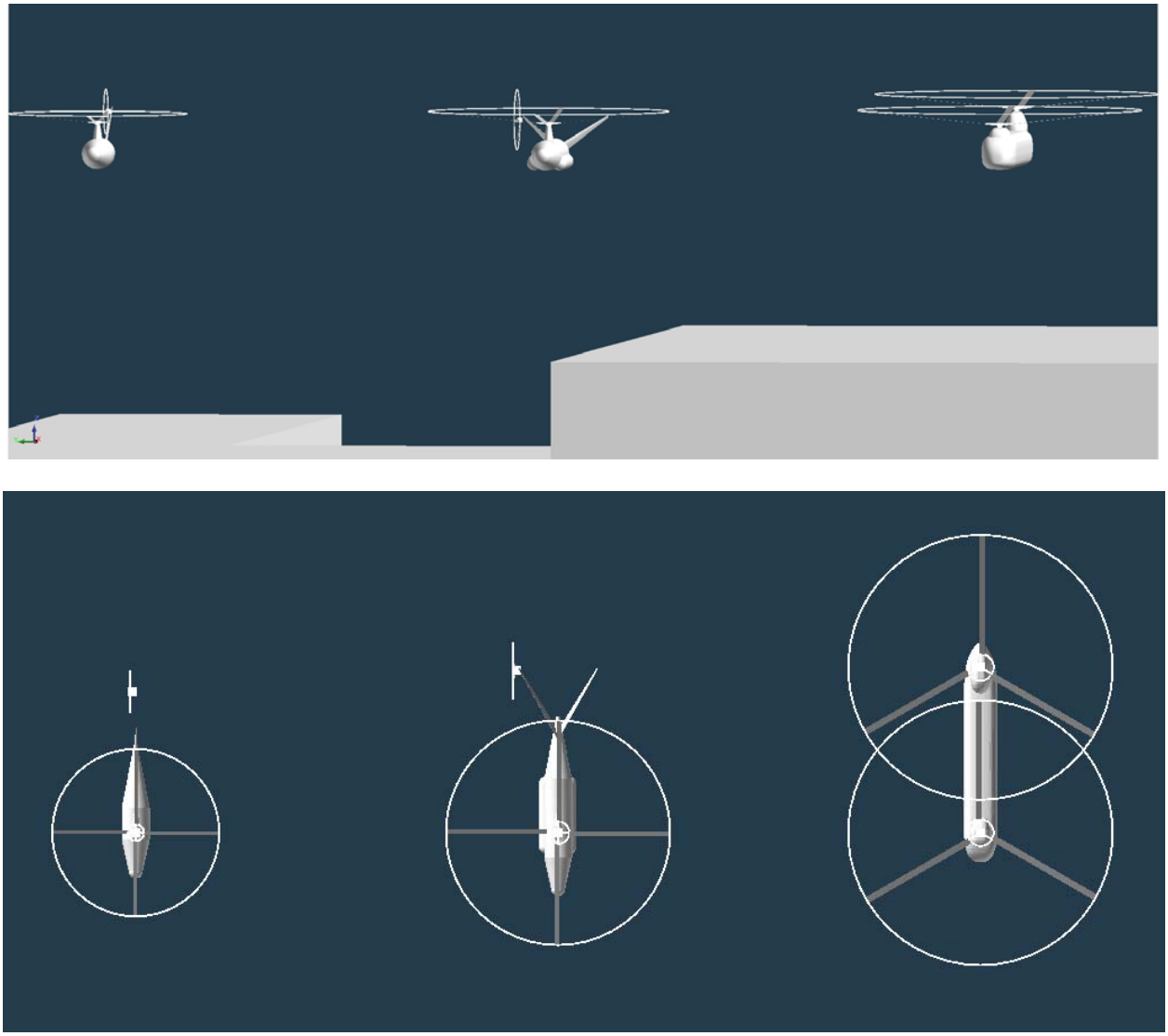

Figure A5. Hopper vehicles incorporated in the BaySim simulations: (a) orthogonal view and (b) planform view.

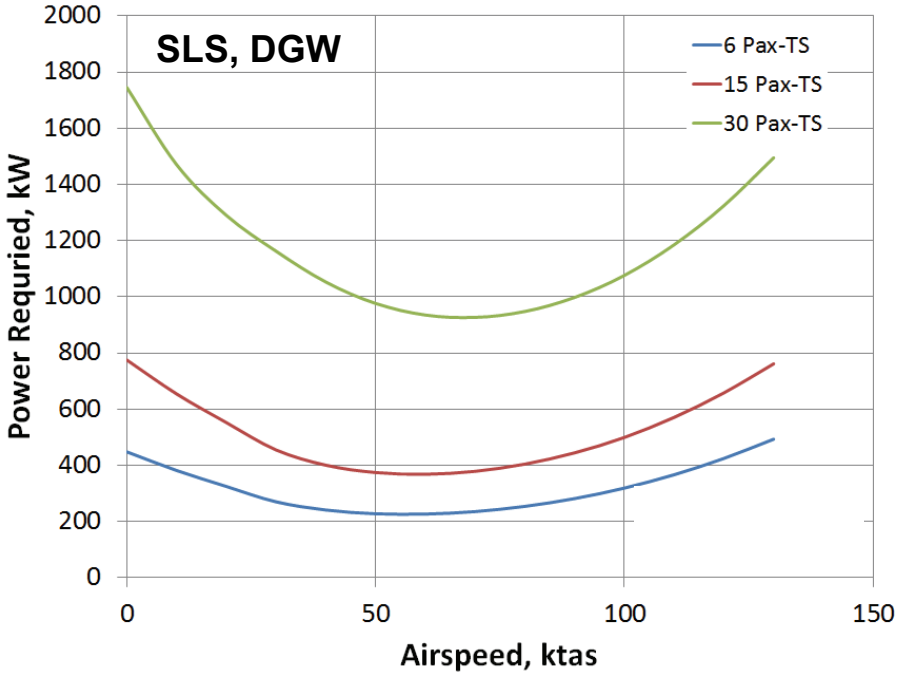

Figure A6. Power trends for three Hopper vehicle sizes.